Simulations, Clusters of Galaxies, and Cosmology: I. Introduction and Large-scale Structure Simulations

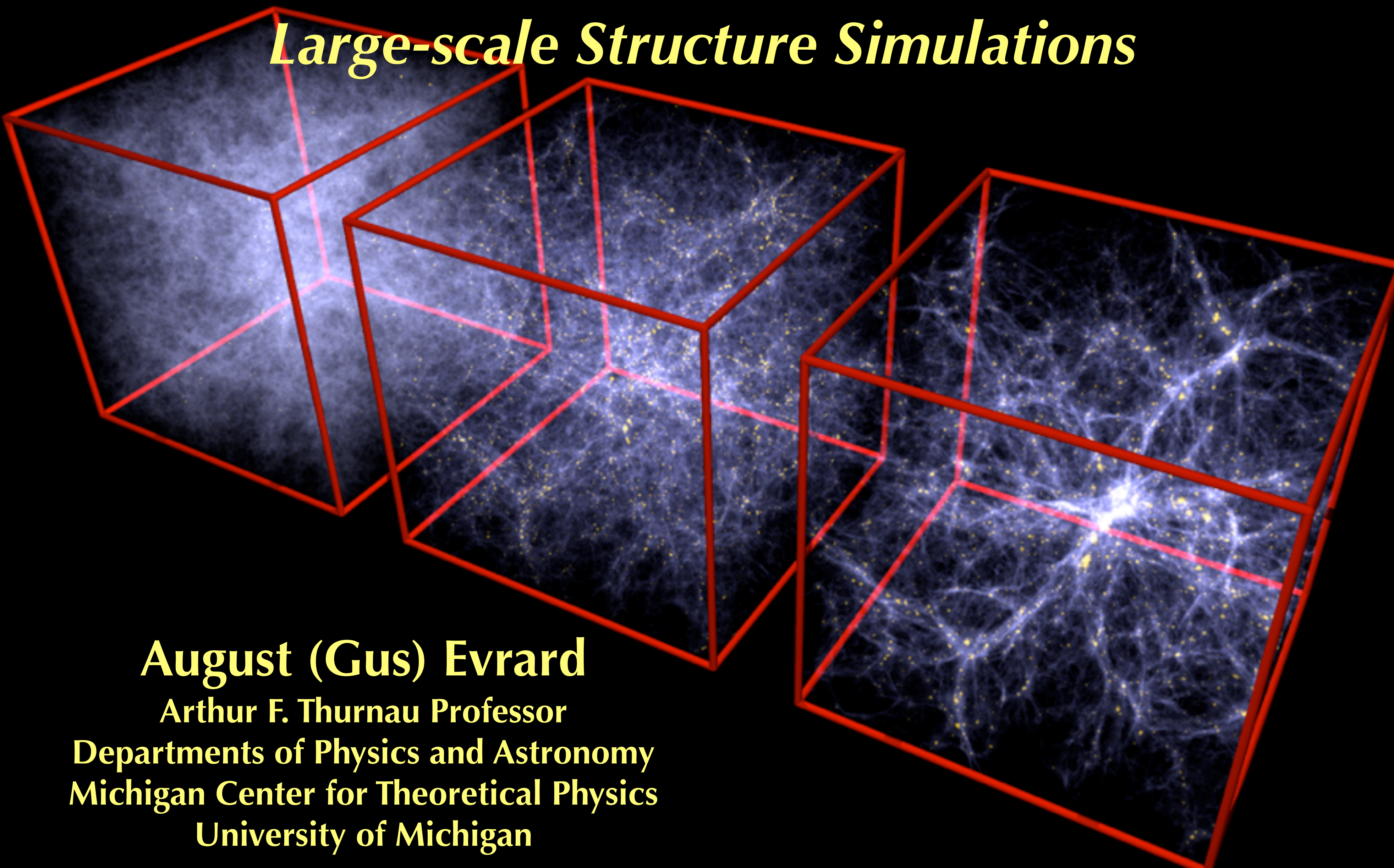

August (Gus) Evrard
Arthur F. Thurnau Professor
Departments of Physics and Astronomy
Michigan Center for Theoretical Physics
University of Michigan

V. Springel & Virgo Consortium 2003

N-body + gas dynamics

multi-fluid systems: N-body+gas dynamics

* baryon fluid coupled via gravity to DM

* solve Euler equation in comoving coordinates

* energy or entropy equation

* requires shock treatment

Bertschinger 1998

In comoving coordinates, the cosmological fluid equations are

$$\frac{\partial}{\partial t}\left(\frac{\rho_b}{\bar{\rho}_b}\right) + \frac{1}{a}\vec{\nabla}\cdot\vec{v}_b = 0,$$

$$\frac{\partial \vec{v}_b}{\partial t} + \frac{1}{a}\vec{v}_b\cdot\vec{\nabla}\vec{v}_b + H\vec{v}_b = -\frac{1}{a\rho_b}\vec{\nabla}p + \vec{g}, \qquad (3)$$

where ρ_b, $\bar{\rho}_b$, $\vec{v}_b$, and p are the (baryonic) mass density, mean mass density, peculiar velocity, and pressure, respectively, and $\vec{g}$ is the gravitational field (Equation 1). These must be supplemented by either an energy or entropy equation. Outside of shocks, these take the form

$$\frac{\partial u}{\partial t} + \frac{1}{a}\vec{v}_b\cdot\vec{\nabla}u = -\frac{p}{a\rho_b}\vec{\nabla}\cdot\vec{v}_b + \frac{1}{\rho_b}(\Gamma - \Lambda),$$

$$\frac{\partial S}{\partial t} + \frac{1}{a}\vec{v}_b\cdot\vec{\nabla}S = \frac{1}{p}(\Gamma - \Lambda). \qquad (4)$$

For a perfect gas with ratio of specific heats γ, the thermal energy and entropy per unit mass are $u = p/[(\gamma-1)\rho_b]$ and $S = (\gamma-1)^{-1}\ln(p\rho_b^{-\gamma})$, respectively. Artificial viscosity is often added to Equation 4 to generate the entropy needed across shock waves. In nonadiabatic calculations, heating and cooling rates per unit volume Γ and Λ and all they depend on, such as ionization and chemistry rate equations, radiative transfer, etc, must be included.

hydro solution methods: various flavors

method	character	advantages	disadvantages	examples
Lagrangian (particle)	•solve energy eq'n along streamlines •local kernel density estimates	•simple, fast •good dynamic range w/ variable kernel scale	•approx. shock treatment •poor error control (no grid)	smoothed particle hydro (SPH) • gadget • gasoline
Eulerian fixed mesh	•uniform (cubic) spatial grid	•simple, fast •good (trunc.) error control •shocks	•limited spatial resolution	• c.f., Kang et al (1994)
Eulerian Adaptive Mesh Refi. (AMR)	•grid cells refined (sub-divided) in target regions	•improved spatial and mass resol'n •wider dynamic range	•complex to code •sensitive to sub-grid handling	• ART • Enzo • RAMSES • FLASH
Moving Mesh	•hybrid Lagr./Eul. •deformable, moveable grid cells (up to max.)	•best of breed?	•very complex to code	•Arepo

goal: halos (and large sub-halos) should contain baryonic objects like this!

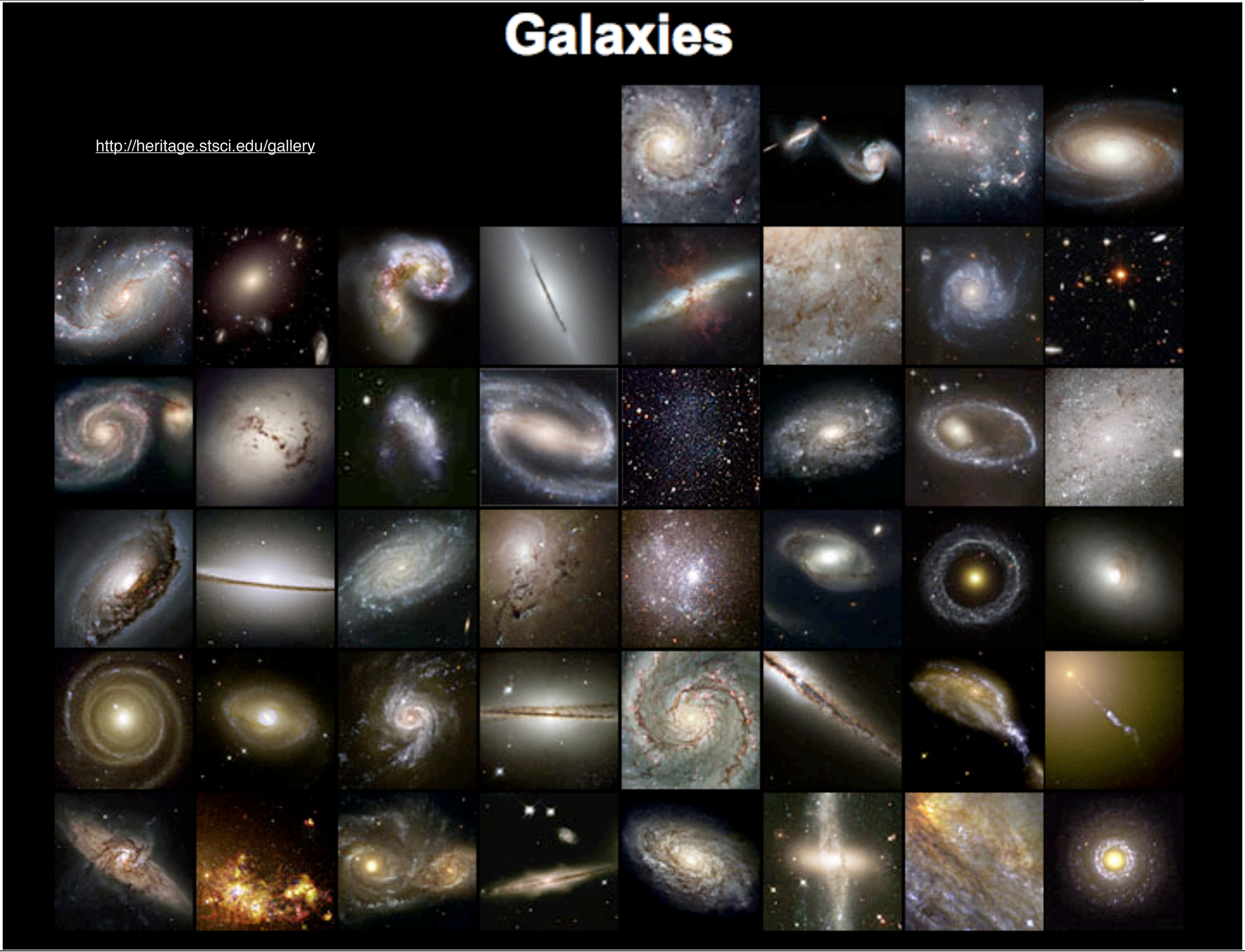

early results with P3MSPH

- 16 Mpc cube in Ω_m=1 universe (aka, SCDM)
- 2 x 64^3 particles on CRAY Y-MP (@SDSC)
- DM $m_p \approx$1e9 Msun, baryon $m_p \approx$1e8 Msun, soft≈10kpc
- shock heating + radiative cooling only

Evrard, Summers and Davis (1994)

z = 6.6

all dark matter

all baryons

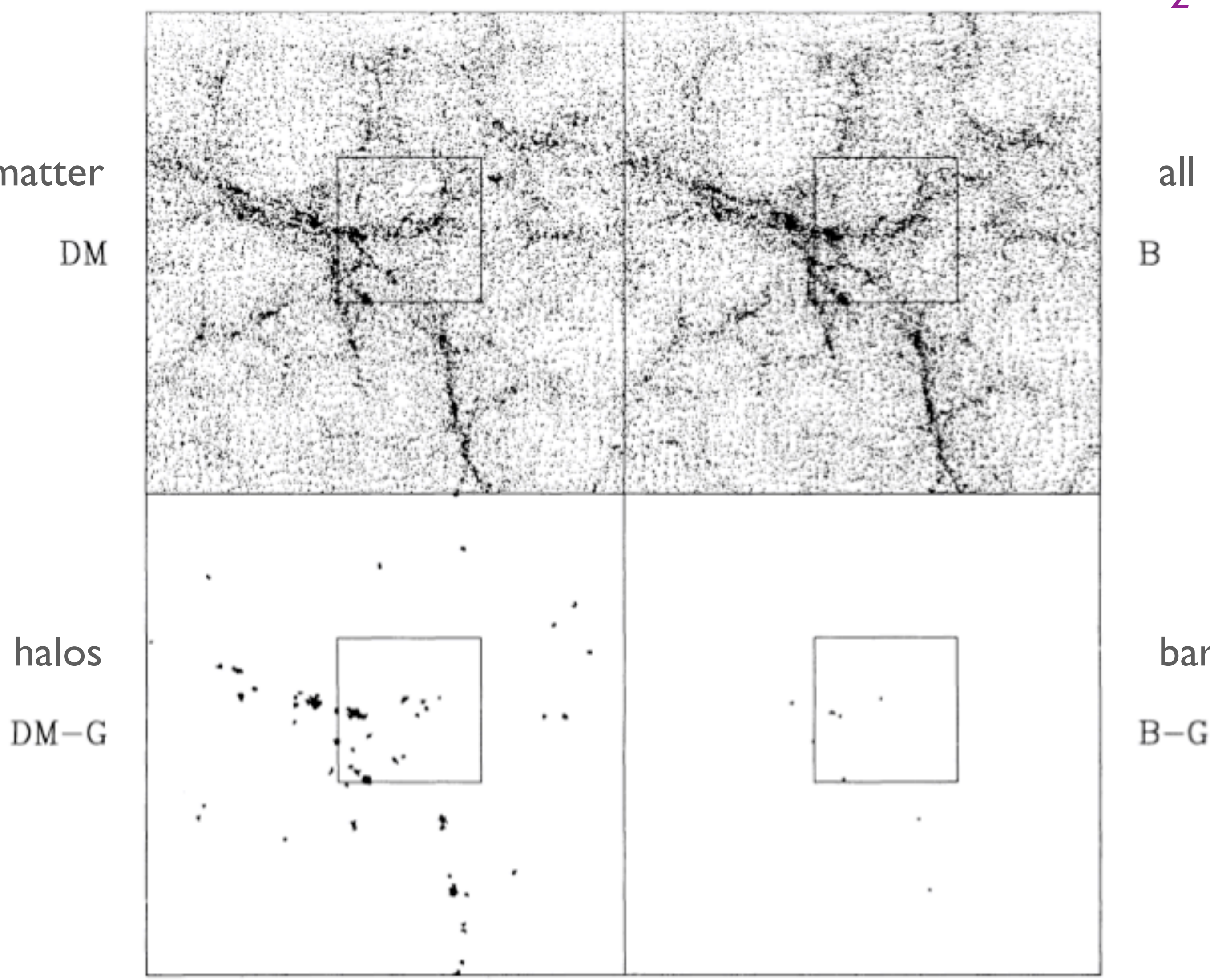

dark matter in halos

baryons in \`globs'

FIG. 1*a*

early results with P3MSPH

- 16 Mpc cube in Ω_m=1 universe (aka, SCDM)
- 2 x 64^3 particles on CRAY Y-MP (@SDSC)
- DM $m_p \approx$1e9 Msun, baryon $m_p \approx$1e8 Msun, soft≈10kpc
- shock heating + radiative cooling only

Evrard, Summers and Davis (1994)

z = 3.0

all dark matter

all baryons

dark matter in halos

baryons in `globs'

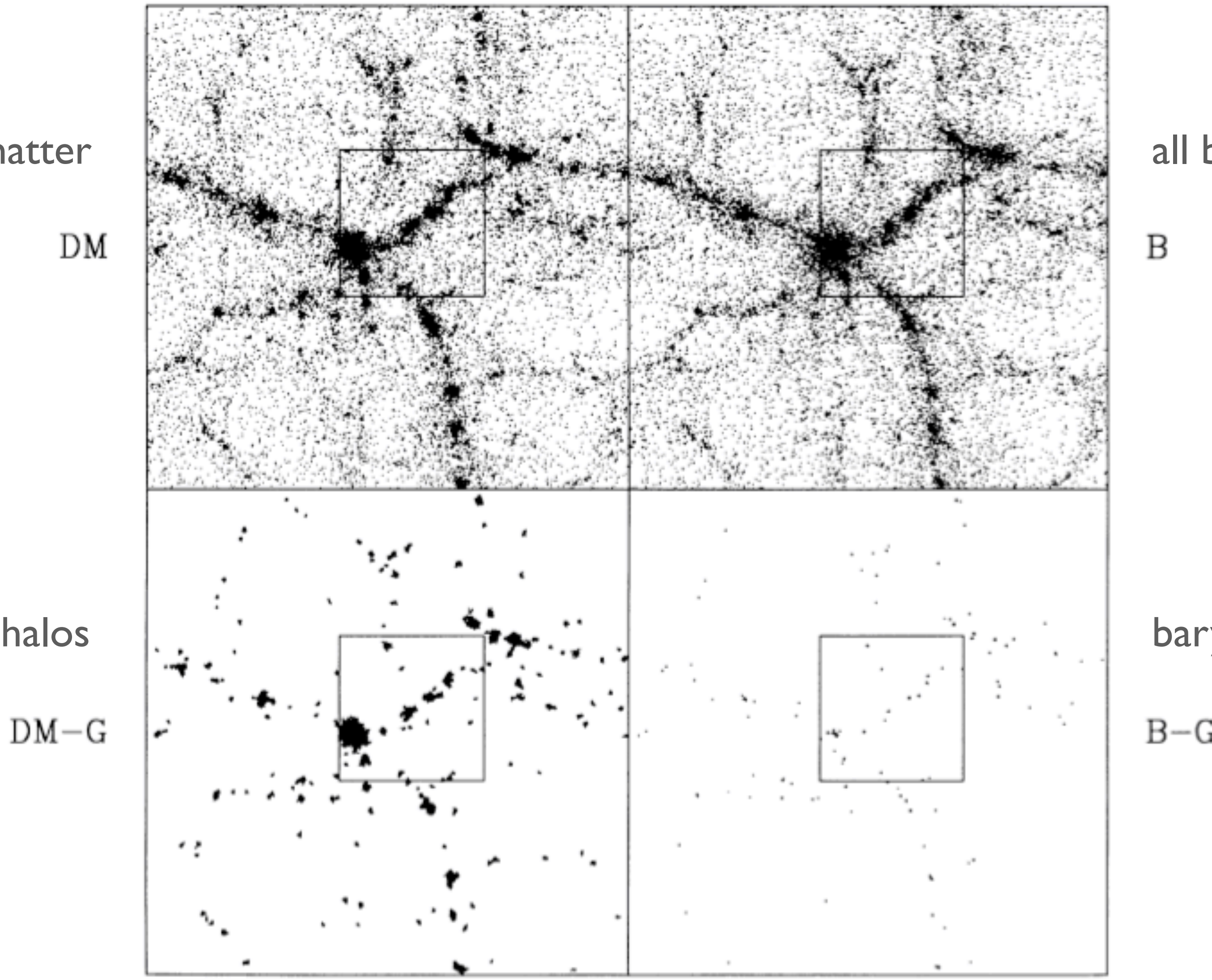

FIG. 2a

early results with P3MSPH

- 16 Mpc cube in Ω_m=1 universe (aka, SCDM)
- 2 x 64^3 particles on CRAY Y-MP (@SDSC)
- DM m_p≈1e9 Msun, baryon m_p≈1e8 Msun, soft≈10kpc
- shock heating + radiative cooling only

Evrard, Summers and Davis (1994)

z = 3.0
(zoom in)

all dark matter

all baryons

dark matter in halos

baryons in `globs'

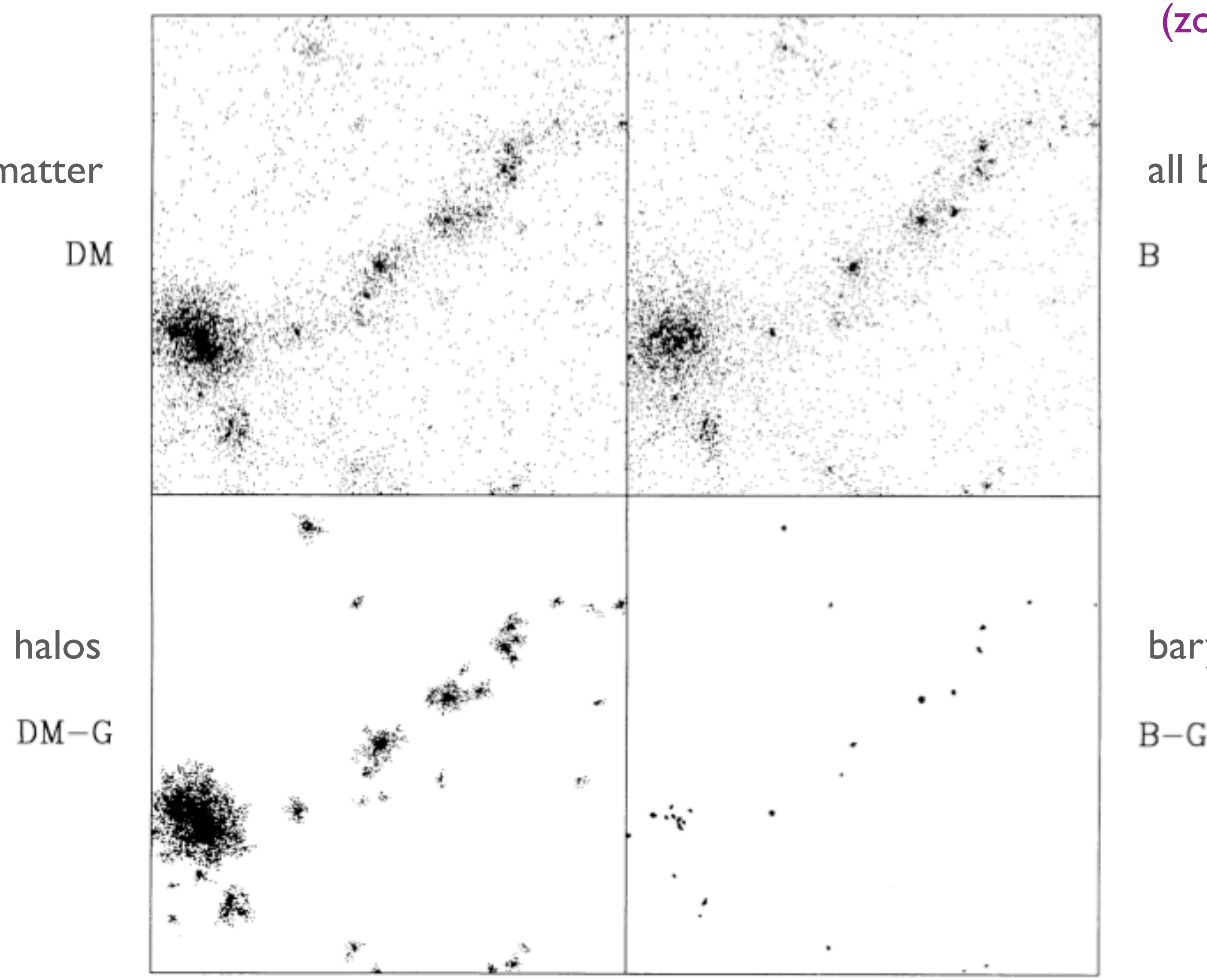

FIG. 2*b*

early results with P3MSPH

- 16 Mpc cube in Ω_m=1 universe (aka, SCDM)
- 2 x 64^3 particles on CRAY Y-MP (@SDSC)
- DM $m_p \approx$1e9 Msun, baryon $m_p \approx$1e8 Msun, soft≈10kpc
- shock heating + radiative cooling only

Evrard, Summers and Davis (1994)

z = 1.0
(zoom in)

all dark matter

all baryons

dark matter in halos

baryons in `globs'

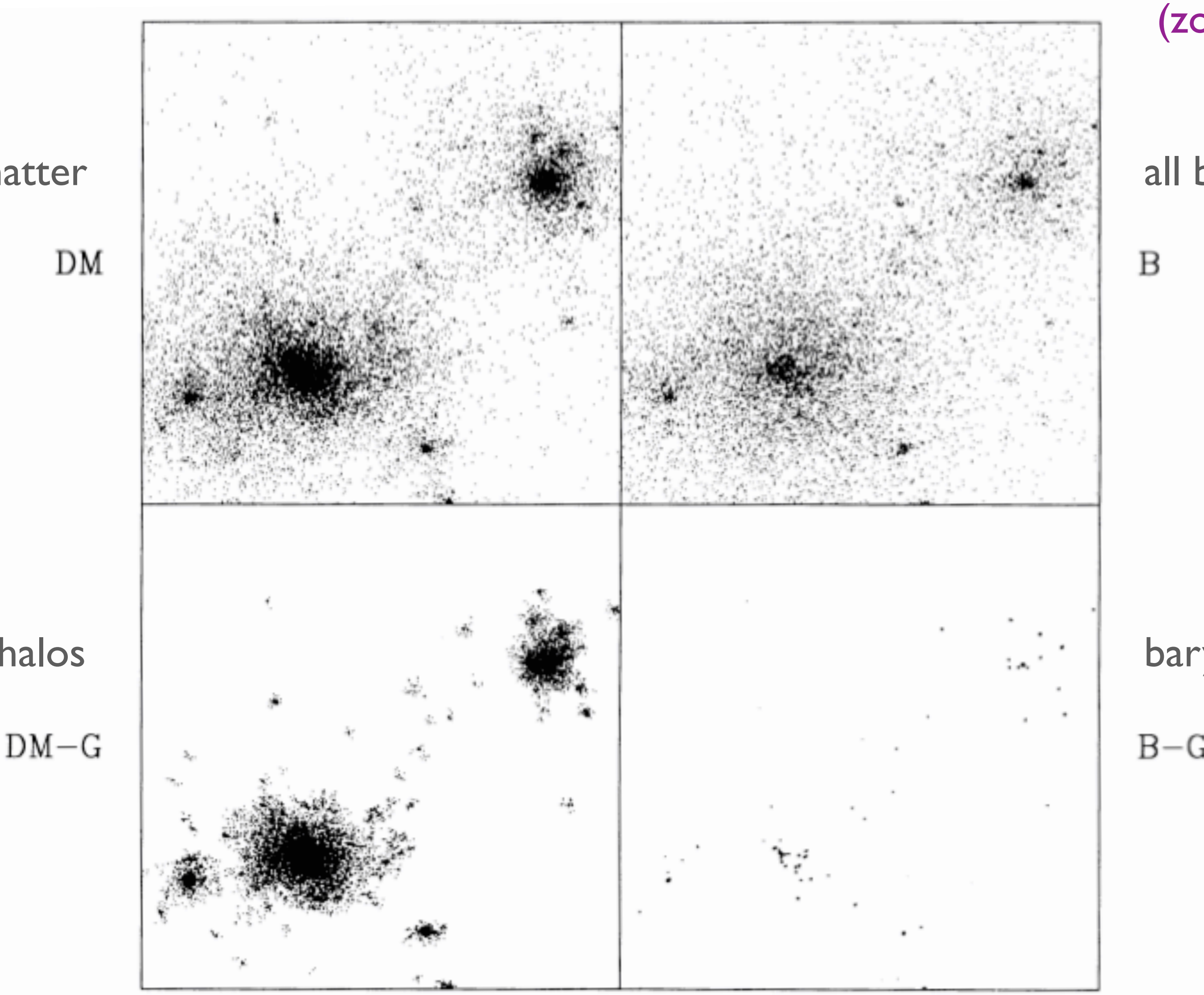

FIG. 3b

early results with P3MSPH

Evrard, Summers and Davis (1994)

phase structure @ z=1

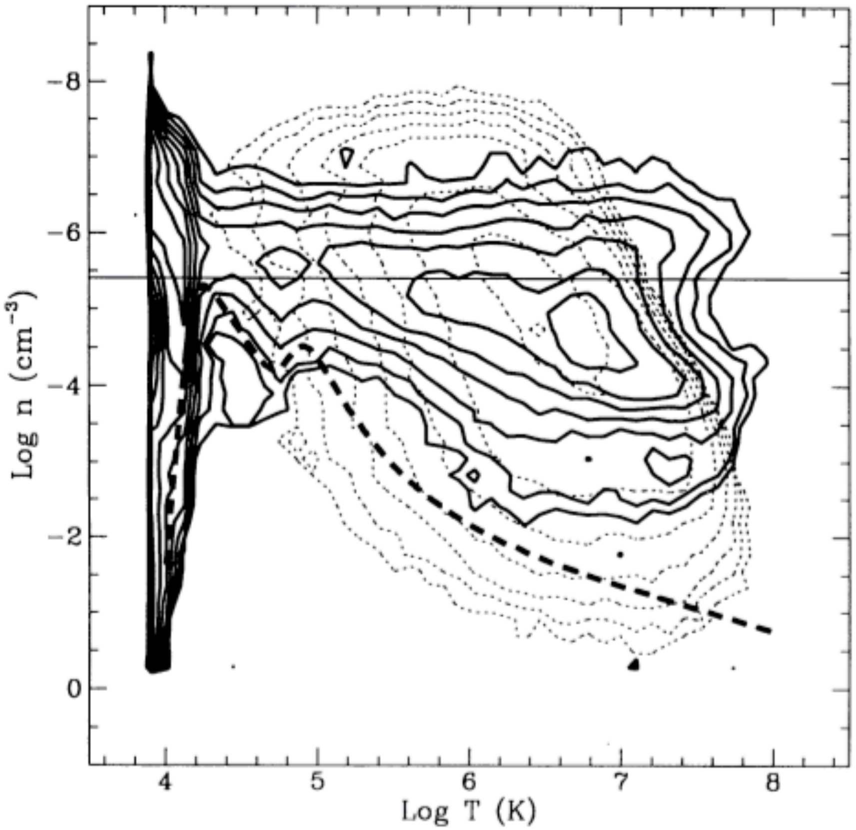

FIG. 4.—Contours of the mass weighted filling factor $f_m(n, T)$ in the density-temperature phase space at $z = 1$. Note the inverted density axis. The minimum contour is at $10^{-3.3}$ and contours are spaced logarithmically at intervals of 0.3. The heavy, dashed line shows the locus of points for which the cooling time equals the final age of the simulation (4.7 Gyr at $z = 1$). The solid contours show the baryon f_m, while the dashed contours show f_m for the dark matter using the specific peculiar kinetic energy.

fraction of cold, dense baryons is resolution-dependent

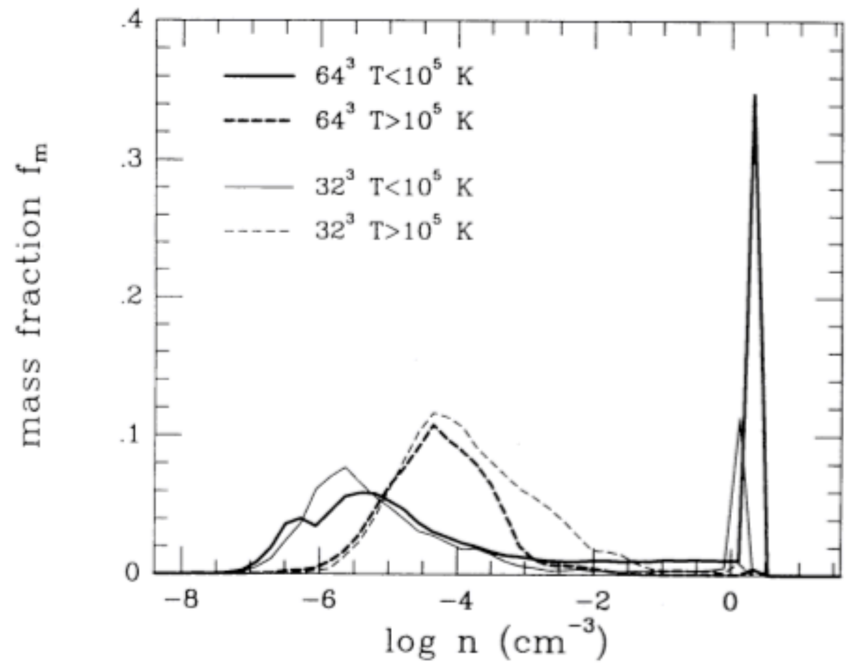

FIG. 5.—One-dimensional filling factors $f_m(n)$ for the cold and hot baryonic phases defined by a separation temperature of 10^5 K. Results are shown both for the 64^3 particle run and a comparison run employing the same (subsampled) initial conditions with 32^3 particles. The fraction of cold, dense baryons is strongly affected by mass resolution.

early results with P3MSPH

Evrard, Summers and Davis (1994)

an early look at the Halo Occupation Distribution (HOD)

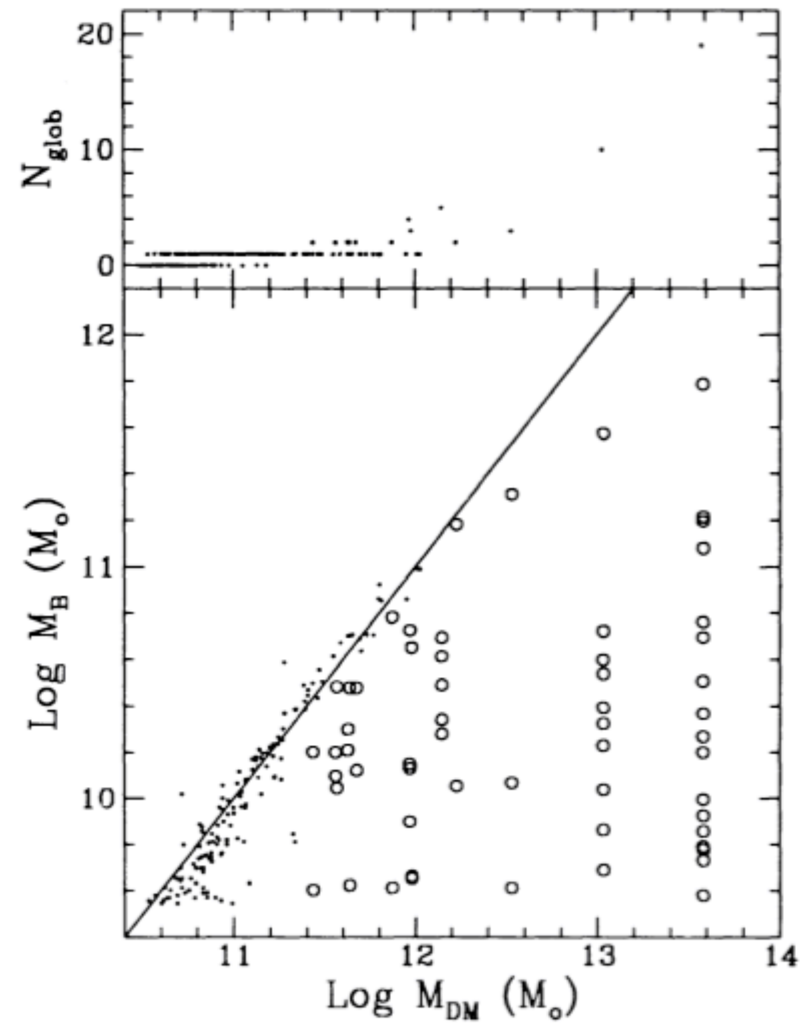

FIG. 11.—Halo occupation number N_{glob} and glob mass within each halo as a function of halo mass. Circles in the lower panel indicate halos containing multiple globs. The line in the lower panel is $M_B = \Omega_b M_{DM}$.

early results with P3MSPH

first cosmological simulation
to form disk galaxies!

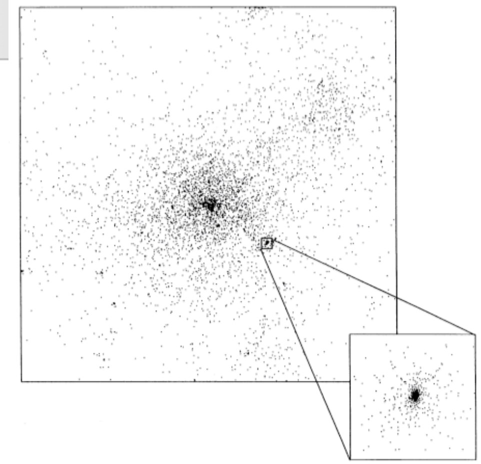

FIG. 17*a*

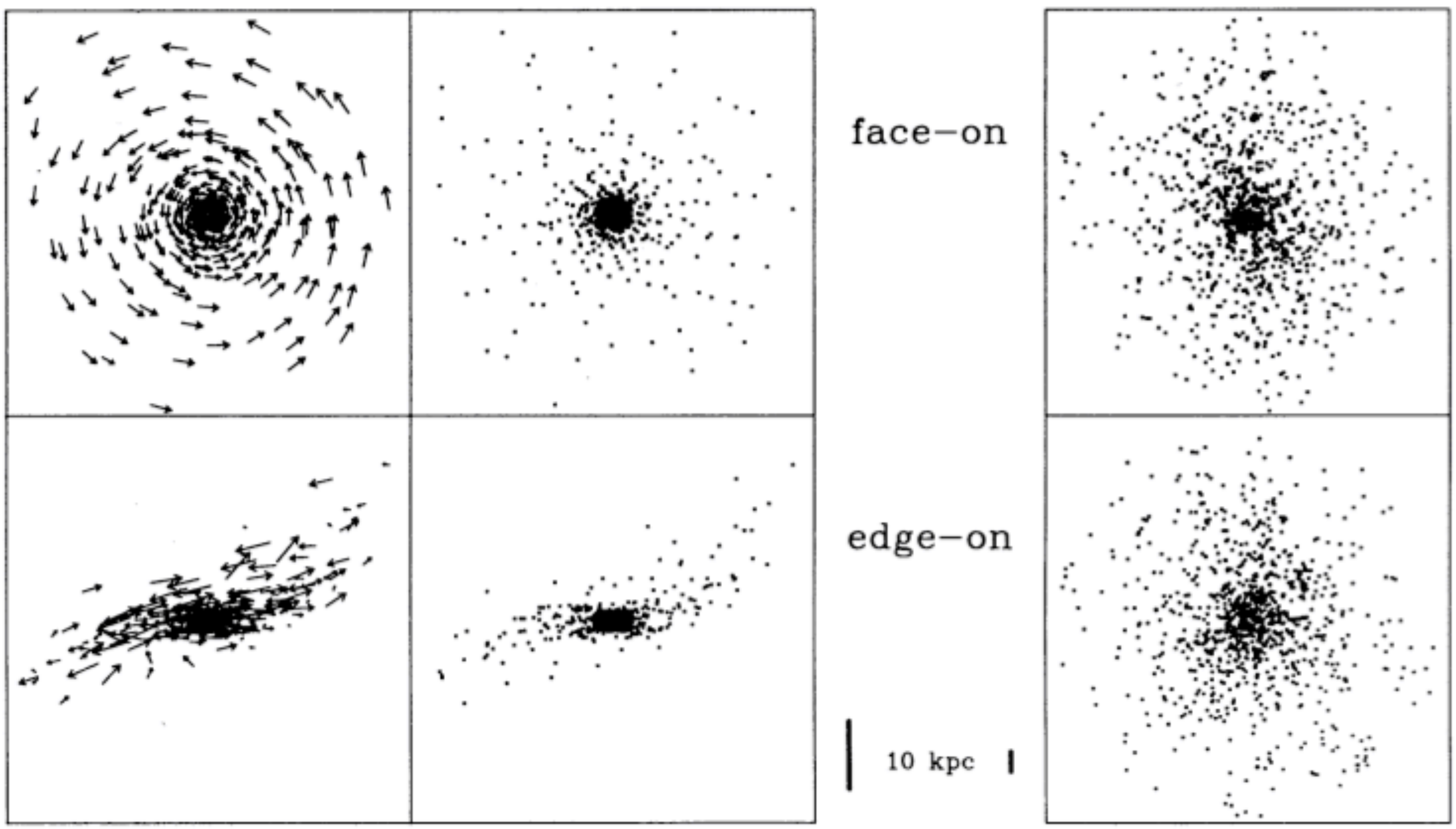

FIG. 17*b*

direct methods for modeling galaxy formation

* direct gas dynamic simulations have evolved to now include
  - radiative cooling based including metal-line cooling
  - star formation prescription based on gas density (+ other properties)
  - local energy and mass feedback from SN
  - metals (C, N, O, Si, ...) from different SN types
  - prescriptions for black hole (BH) accretion and merging
  - feedback from central galactic BH's
  - stellar population synthesis model to predict optical-IR properties
  - +... (more every year)

x

baryon physics available in current codes

Benson (2010)

Table 1: A survey of physical processes included in several of the major hydrodynamical codes. The primary reference is indicated next to the name of the code. Where implementations of major physical processes are described elsewhere the reference is given next to the entry in the relevant row.

Feature	GADGET-3[1]	GASOLINE[2]	HART[3]	ENZO(ZEUS)[4]	FLASH[5]
Gravity	Tree	Tree	AMR[6] PM[7]	AMR[6] PM[7]	Multi-grid
Hydrodynamics	SPH[8]	SPH[8]	AMR[6]	AMR[6]	AMR[6]
→ Multiphase subgrid model[9]	✓[10]	×	N/A	N/A	N/A
Radiative Cooling	✓	✓	✓	✓	✓[11]
→ Metal dependent	✓[12]	×	✓[13]	✓[14]	✓[11]
→ Molecular chemistry	✓[15]	×	✓[13,16]	✓[17]	×
Thermal Conduction	✓[18]	×	×	×	✓
Star formation	✓[19]	✓[20]	✓[13]	✓[21]	×
→ SNe feedback	✓[19]	✓[20]	✓[13]	✓[21]	×
→ Chemical enrichment	✓[19]	✓[20]	✓[13]	✓[21]	×
Black hole formation	✓[22]	×	×	×	✓[23]
→ AGN feedback	✓[22]	×	×	×	×
Radiative transfer	OTVET[24,25]	×	OTVET[24]	✓[26]	✓[27]
Magnetic fields	✓[28]	×	×	✓[29]	✓[30]

Notes

[1] "GAlaxies with Dark matter and Gas intEracT" (Springel, 2005);
[2] Wadsley et al. (2004);
[3] Hydrodynamic Adaptive Refinement Tree (Kravtsov et al., 2002);
[4] O'Shea et al. (2004);
[5] `http://flash.uchicago.edu` (Fryxell et al., 2000);
[6] Adaptive Mesh Refinement;
[7] Particle–mesh;
[8] Smoothed Particle Hydrodynamics;
[9] Applicable only to SPH codes—used correctly, AMR codes naturally resolve multiphase media;
[10] Scannapieco et al. (2006a);
[11] Banerjee et al. (2006);
[12] Scannapieco et al. (2005);
[13] Tassis et al. (2008);
[14] Smith et al. (2009);
[15] Yoshida et al. (2003);
[16] Equilibrium only;
[17] Turk (2009);
[18] Jubelgas et al. (2004);
[19] Scannapieco et al. (2005);
[20] Governato et al. (2007);
[21] Tasker and Bryan (2008);
[22] Matteo et al. (2005);
[23] Federrath et al. (2010);
[24] Optically Thin Variable Eddington Tensor;
[25] Petkova and Springel (2009);
[26] Flux-limited diffusion approximation (Norman et al. 2009; see also Wise and Abel 2008b);
[27] Rijkhorst et al. (2006); Peters et al. (2010);
[28] Dolag and Stasyszyn (2008);
[29] Collins et al. (2009; see also Wang and Abel 2009);

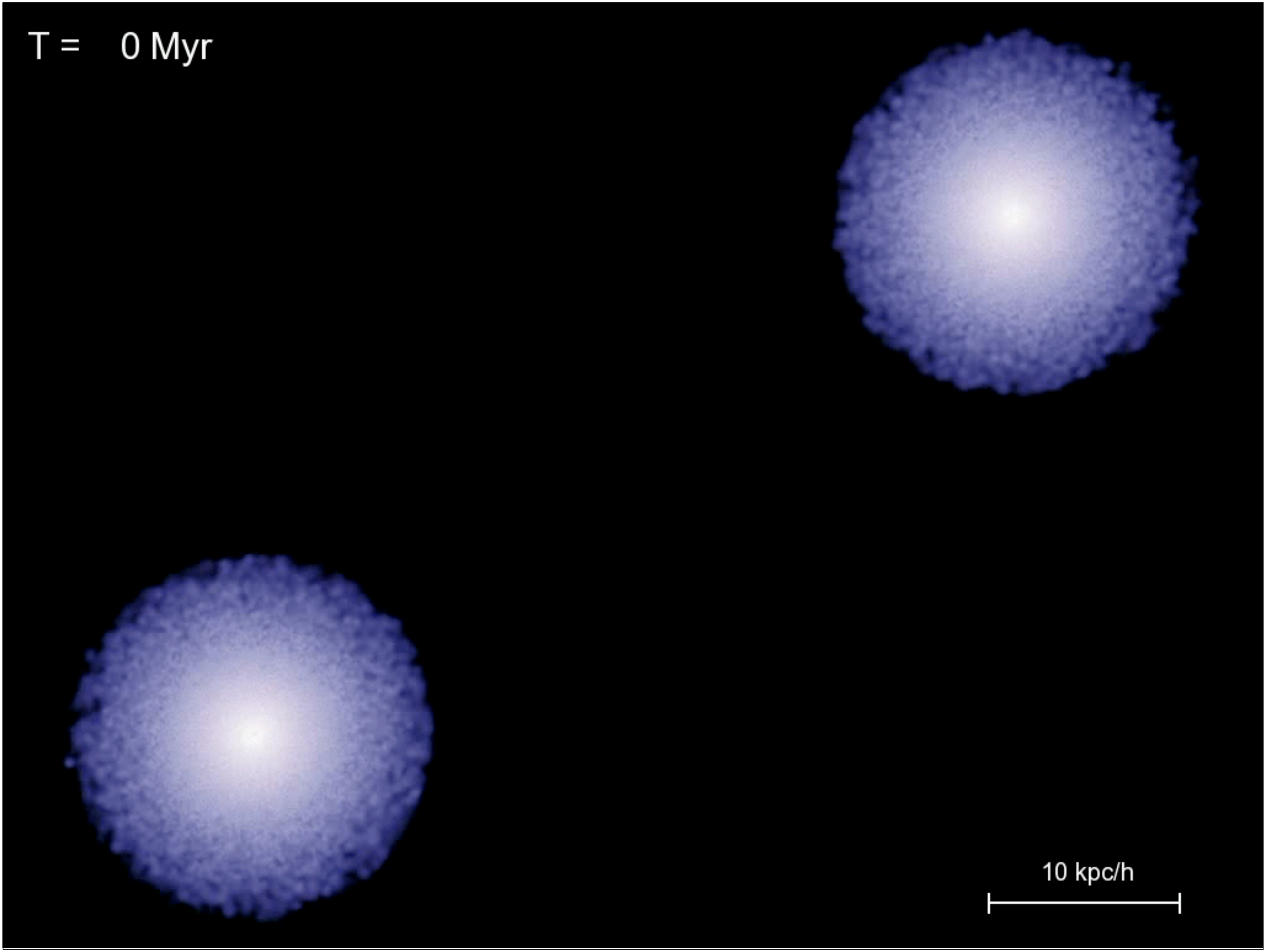
T = 0 Myr
10 kpc/h

effects of AGN feedback on gas and stars in galaxy groups

Battacharya et al (2008)

z=1

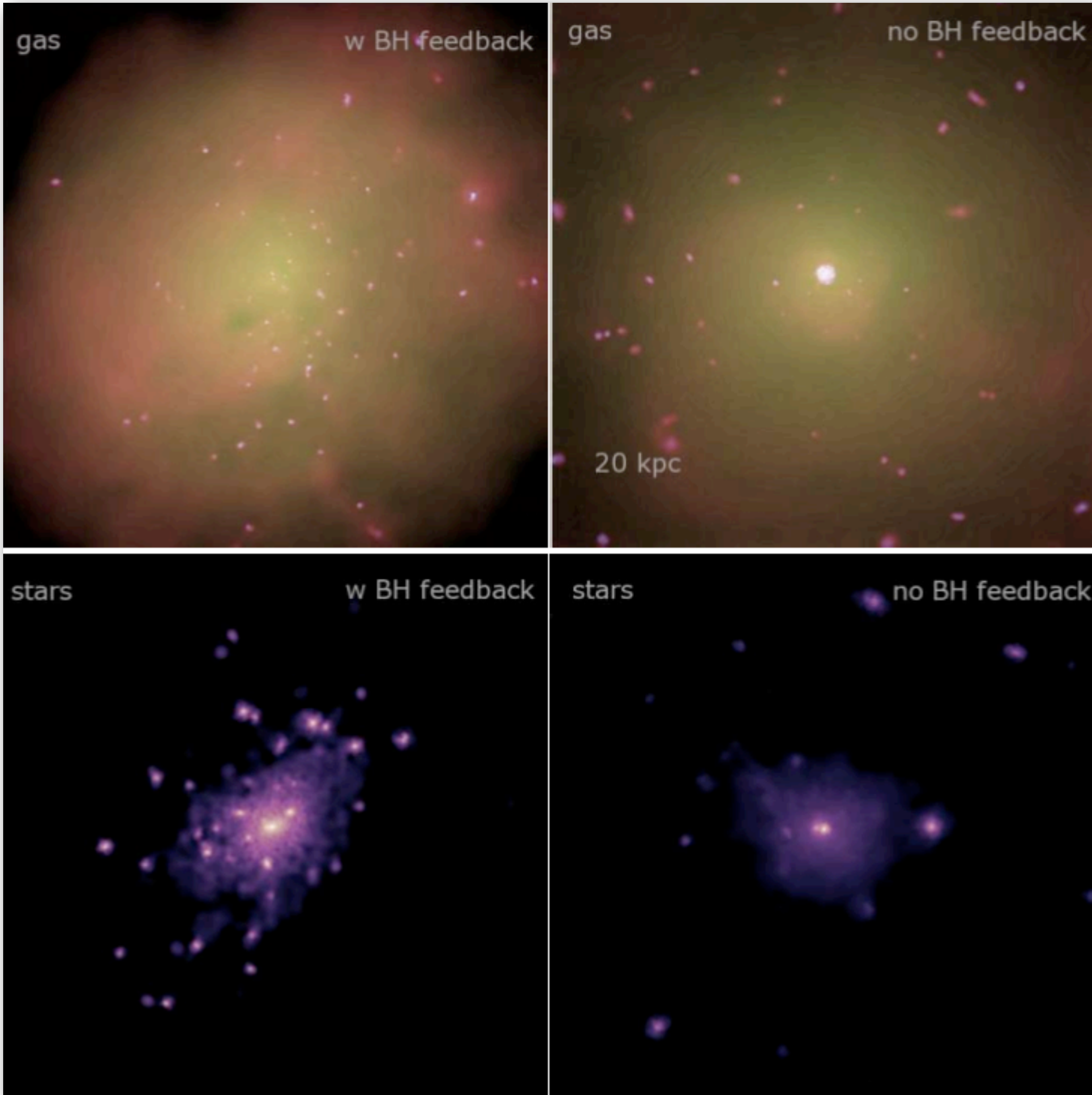

effects of AGN feedback on gas and stars in galaxy groups

Bhattacharya et al (2008)

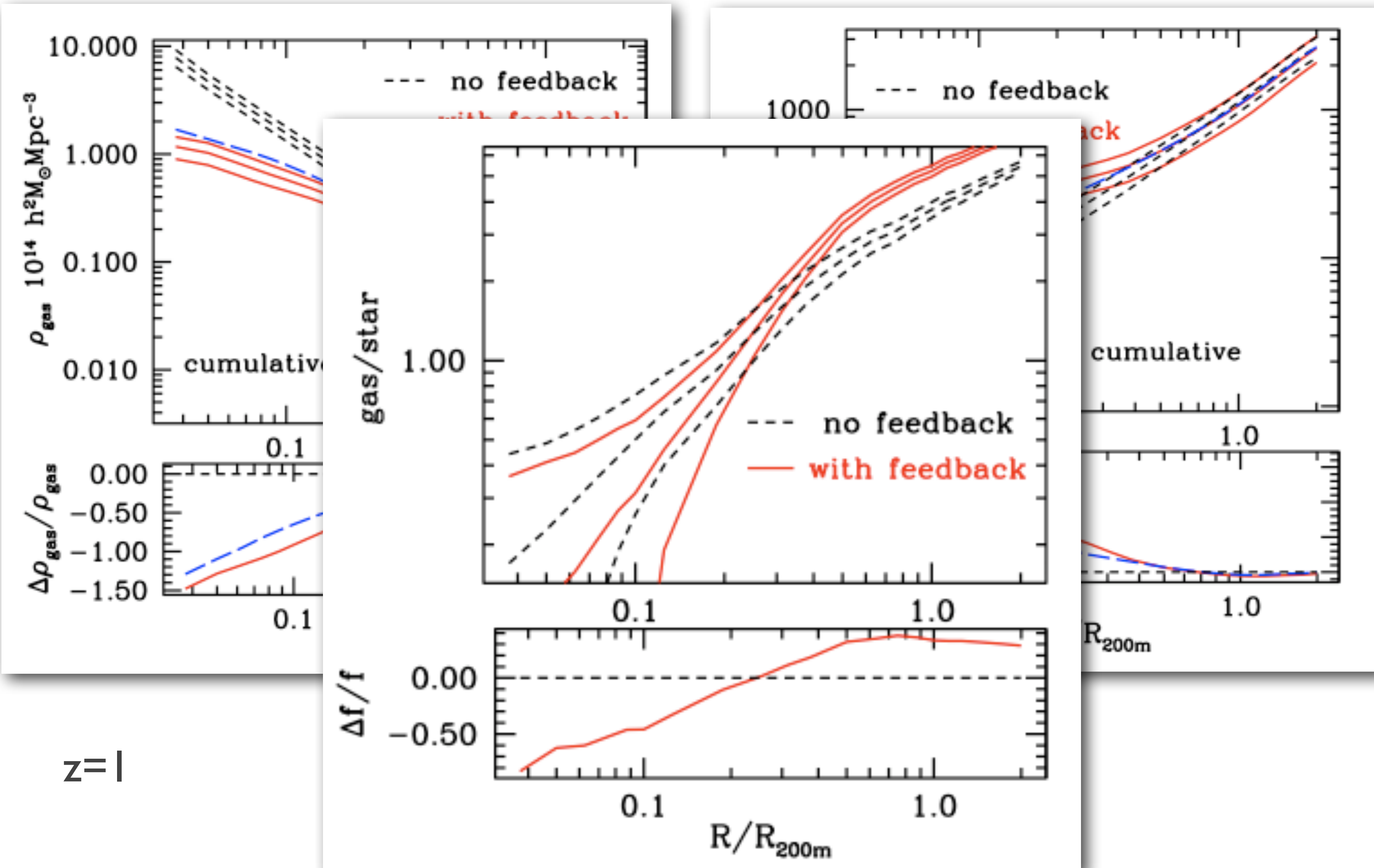

z=1

best effort (circa 2011) at simulating formation of the Milky Way

Guedes et al (2011)

FORMING REALISTIC LATE-TYPE SPIRALS IN A ΛCDM UNIVERSE: THE ERIS SIMULATION

JAVIERA GUEDES[1,3], SIMONE CALLEGARI[2], PIERO MADAU[1], & LUCIO MAYER[2,3]

accepted by the ApJ

ABSTRACT

Simulations of the formation of late-type spiral galaxies in a cold dark matter (ΛCDM) universe have traditionally failed to yield realistic candidates. Here we report a new cosmological N-body/smooth particle hydrodynamic (SPH) simulation of extreme dynamic range in which a close analog of a Milky Way disk galaxy arises naturally. Termed "Eris", the simulation follows the assembly of a galaxy halo of mass $M_{\rm vir} = 7.9 \times 10^{11}$ $M_\odot$ with a total of $N = 18.6$ million particles (gas + dark matter + stars) within the final virial radius, and a force resolution of 120 pc. It includes radiative cooling, heating from a cosmic UV field and supernova explosions (blastwave feedback), a star formation recipe based on a high gas density threshold ($n_{\rm SF} = 5$ atoms cm^{-3} rather than the canonical $n_{\rm SF} = 0.1$ atoms cm^{-3}), and neglects any feedback from an active galactic nucleus. Artificial images are generated to correctly compare simulations with observations. At the present epoch, the simulated galaxy has an extended rotationally-supported disk with a radial scale length $R_d = 2.5$ kpc, a gently falling rotation curve with circular velocity at 2.2 disk scale lengths of $V_{2.2} = 214$ km s^{-1}, an i-band bulge-to-disk ratio $B/D = 0.35$, and a baryonic mass fraction within the virial radius that is 30% below the cosmic value. The disk is thin, has a typical H I-to-stellar mass ratio, is forming stars in the region of the $\Sigma_{\rm SFR}$-$\Sigma_{\rm HI}$ plane occupied by spiral galaxies, and falls on the photometric Tully-Fisher and the stellar mass-halo virial mass relations. Hot ($T > 3 \times 10^5$ K), X-ray luminous halo gas makes only 26% of the universal baryon fraction and follows a "flattened" density profile $\propto r^{-1.13}$ out to $r = 100$ kpc. Eris appears then to be the first cosmological hydrodynamic simulation in which the galaxy structural properties, the mass budget in the various components, and the scaling relations between mass and luminosity are all consistent with a host of observational constraints. A twin simulation with a low star formation density threshold results in a galaxy with a more massive bulge and a much steeper rotation curve, as in previously published work. A high star formation threshold appears therefore key in obtaining realistic late-type galaxies, as it enables the development of an inhomogeneous interstellar medium where star formation and heating by supernovae occur in a clustered fashion. The resulting outflows at high redshifts reduce the baryonic content of galaxies and preferentially remove low angular momentum gas, decreasing the mass of the bulge component. Simulations of even higher resolution that follow the assembly of galaxies with different merger histories shall be used to verify our results.

Subject headings: galaxies: evolution – halos – kinematics and dynamics – method: numerical

Eris simulation synthetic images in optical-UV

Guedes et al (2011)

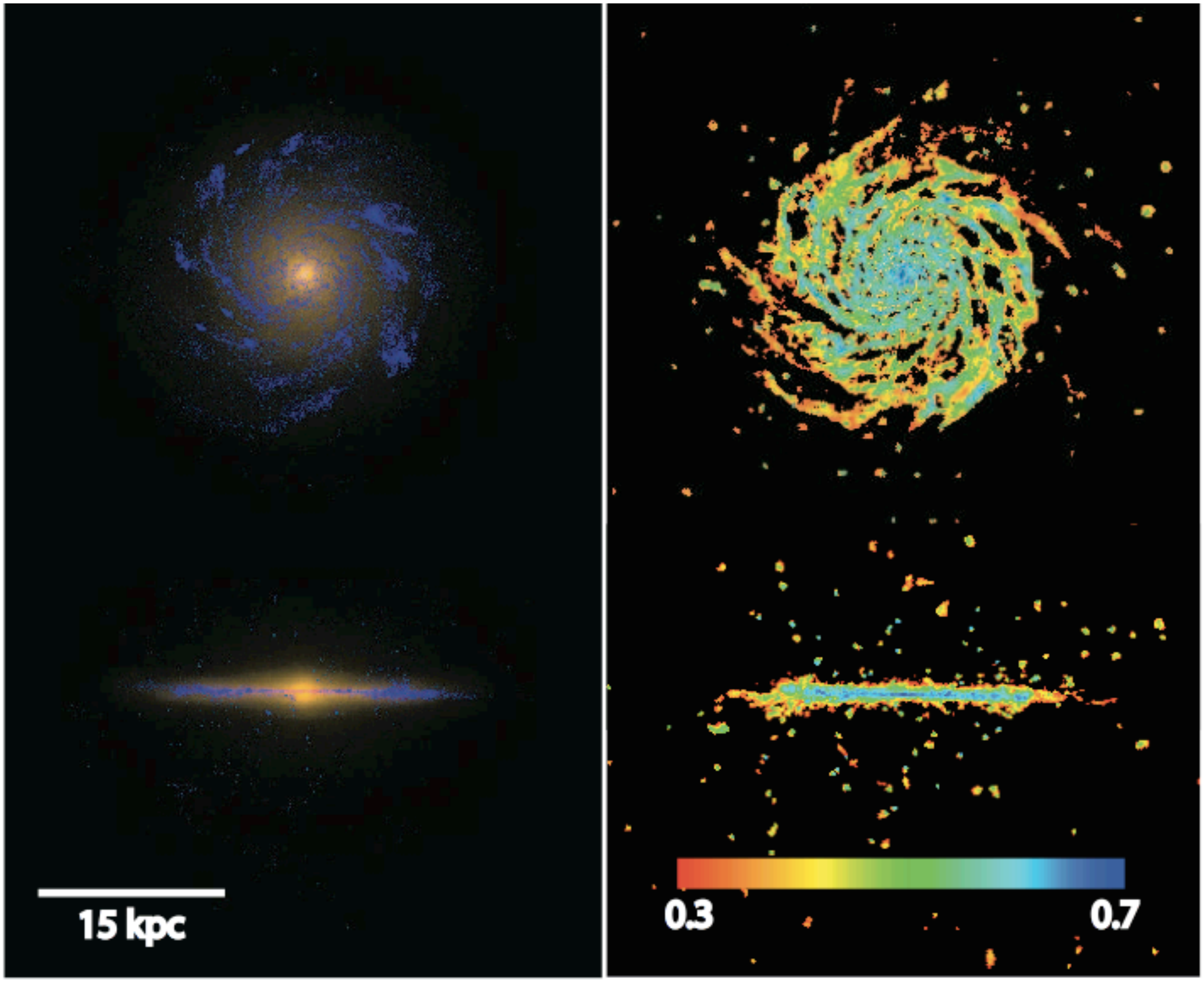

FIG. 2.— *Left panel:* The optical/UV stellar properties of Eris at $z = 0$. The images, created with the radiative transfer code SUNRISE (Jonsson 2006), show an i, V, and FUV stellar composite of the simulated galaxy seen face-on and edge-on. A Kroupa IMF was assumed. *Right panel:* Projected face-on and edge-on surface density maps of Eris's neutral gas at $z = 0$. The color bar shows the neutral gas

Eris simulation galaxy properties are realistic

Guedes et al (2011)

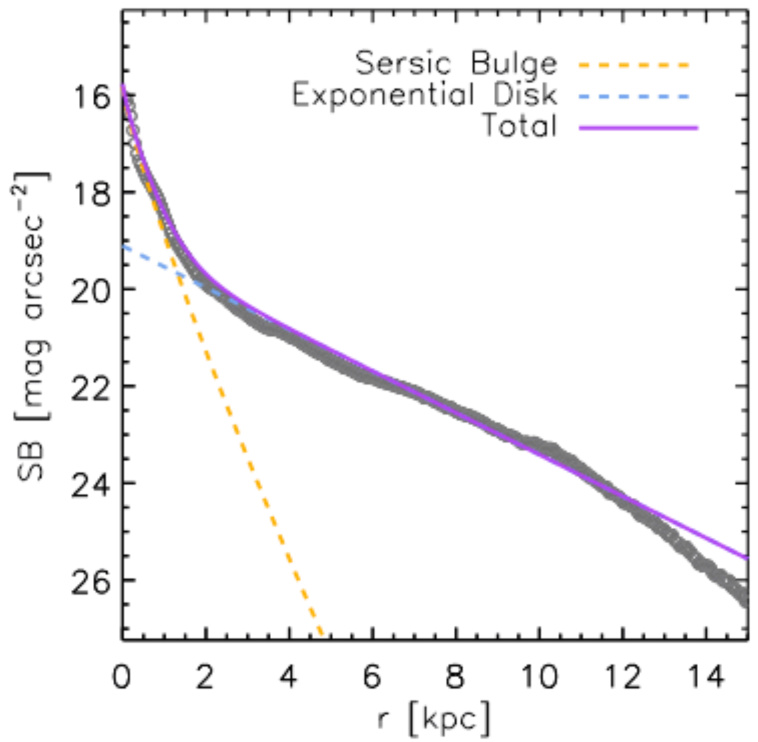

FIG. 3.— The 1D i-band radial surface brightness profile of Eris at $z = 0$. This is well fitted by a Sérsic bulge with index $n_s = 1.4$, an exponential disk with scale length $R_d = 2.5$ kpc, and a bulge-to-disk ratio $B/D = 0.35$. The dust reddened, face-on 2D light distribution created by SUNRISE was analyzed with GALFIT (Peng et al. 2002) following a procedure similar to that detailed in Weinzirl et al. (2009). The "downbending" in the brightness exponential profile at about 5 disk scale length and the surface brightness where the break occurs, 23.5 i-mag arcsec^{-2}, are characteristic of late-type spiral galaxies (Pohlen & Trujillo 2006).

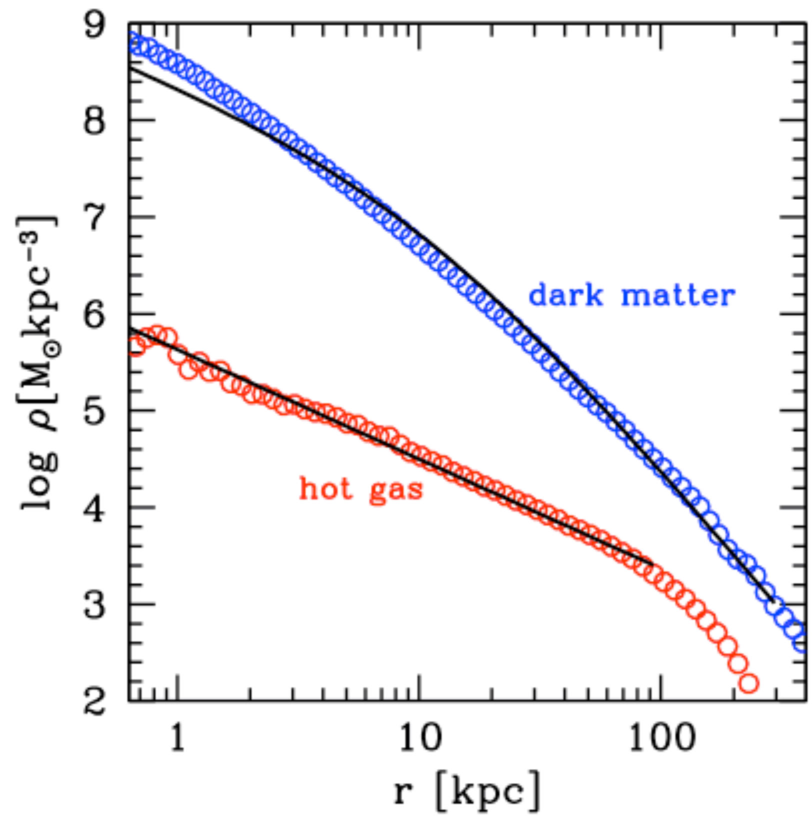

FIG. 5.— The average dark matter (*blue empty dots*) and hot ($T > 3 \times 10^5$ K) gas (*red empty dots*) density profiles of Eris at $z = 0$. The solid lines show the best-fit NFW profile for the dark matter (*upper curve*) and the best-fit power-law profile (with slope -1.13) for the hot gas (*lower curve*). The best-fit NFW profile is characterized by a large halo concentration parameter $c \equiv R_{\rm vir}/R_s = 22$ as the dark matter halo contracts in response to the condensation of baryons in its center.

Eris simulation: low baryon fraction with new star formation parameters

Guedes et al (2011)

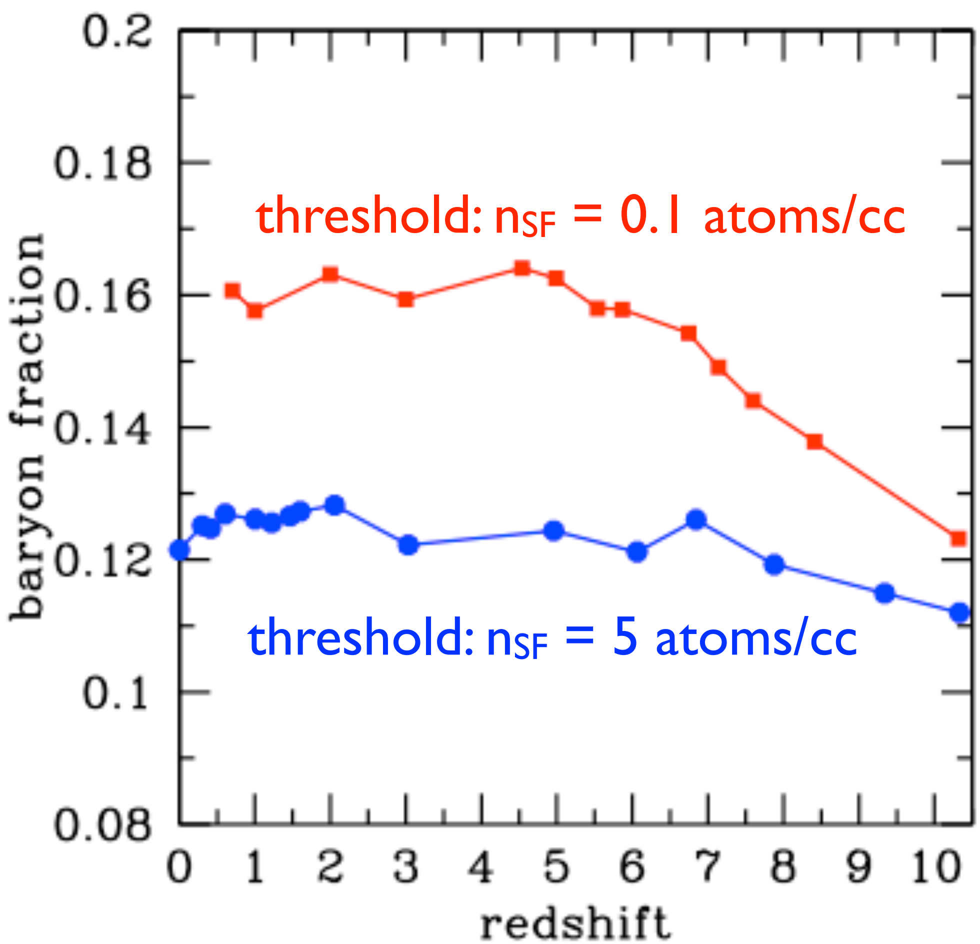

Eris simulation galaxy properties appear realistic

Guedes et al (2011)

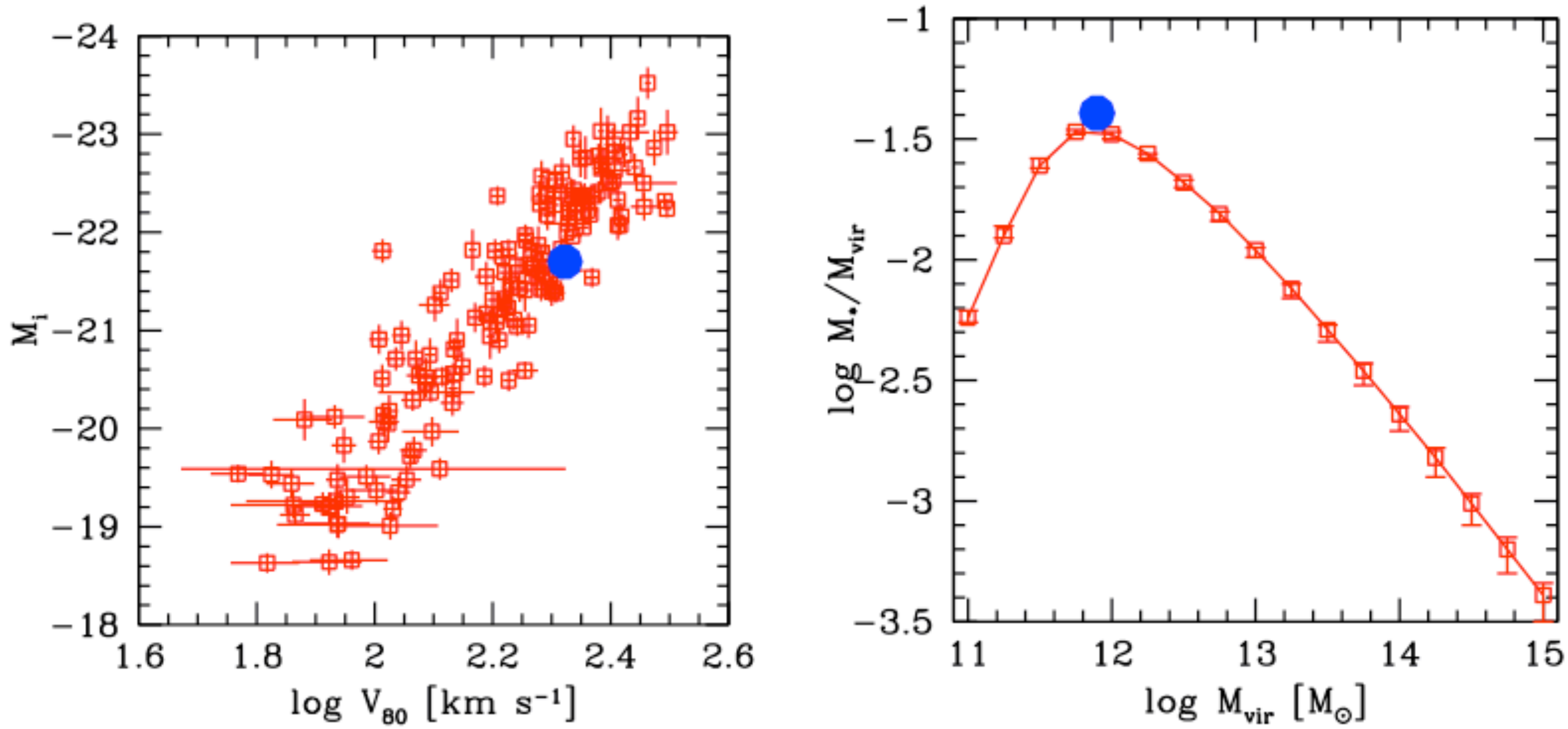

FIG. 4.— *Left panel:* The *i*-band Tully-Fisher relation for the Pizagno et al. (2007) galaxy sample (*empty squares with error bars*). *Filled circle:* The Eris simulation. Here V_{80} denotes the circular velocity at the radius containing 80% of the *i*-band flux, as defined by Pizagno et al. (2007). *Right panel:* The stellar mass - halo mass relation at $z = 0.1$ from Behroozi et al. (2010), modified for a Kroupa IMF (*empty squares with error bars*). Errors bars include only statistical uncertainties. *Filled circle:* The Eris simulation with a photometric stellar mass of $\mathcal{M}_* = 3.2 \times 10^{10}$ $M_\odot$ and a virial mass of $M_{vir} = 7.9 \times 10^{11}$ $M_\odot$ (see text for details).

indirect methods for modeling galaxy formation

Cole (2000)
Benson (2010)

* alternative/complementary approach: Semi-analytic models (SAM's)
  - basic idea: turn PDE problem into simpler ODE problem
  - track halo/sub-halo evolution in DM-only simulation
  - use formation history to determine T, ρ of enclosed gas
  - compute cooling, star formation, heating within halo/sub
  - apply rules for behavior of gas+stars during mergers
  - output: baryon content + star/BH formation history for each halo/sub
  - add stellar population synthesis model to predict optical-IR properties

process view of SAM's

1) input cosmology and astrophysics

2) generate merger tree realization (via N-body or analytically)

3) turn crank

4) compare output to observations

(write papers...)

5) adjust inputs and return to step 1)

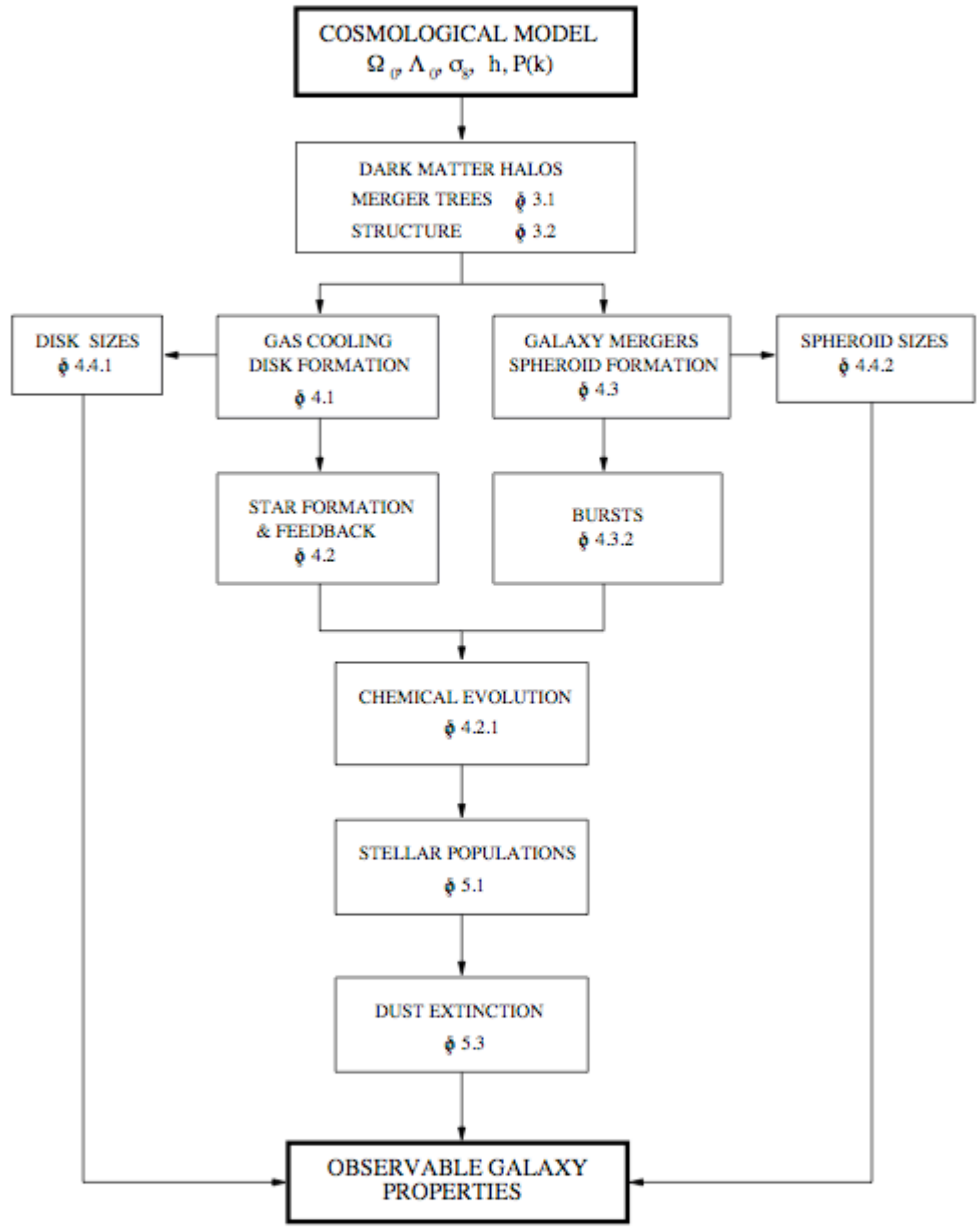

Cole (2000)

SAM produce rich phenomenology

Cole (2000)

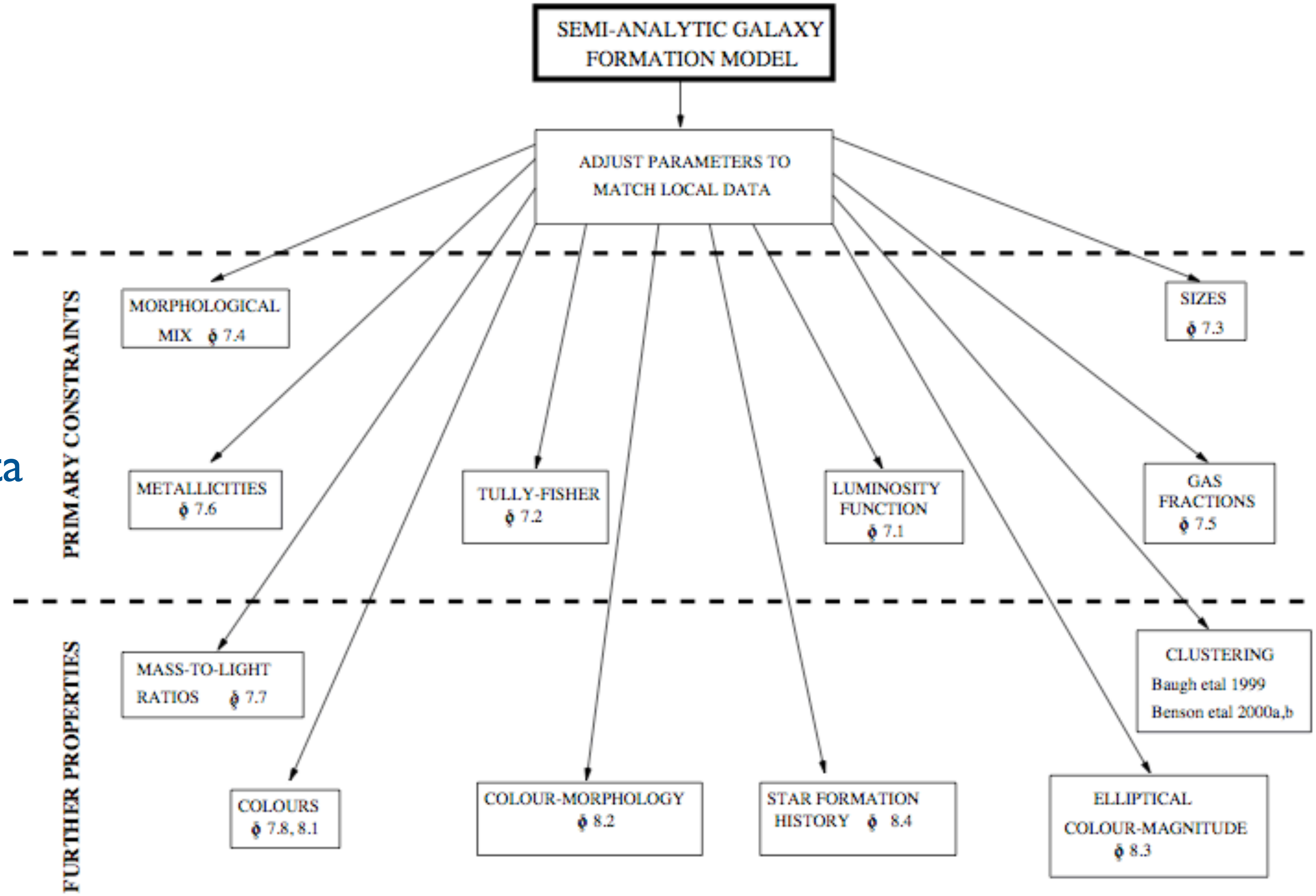

tune to match `low-order' data

then predict `higher-order' data

SAM: tracking of multi-phase gas and stellar behavior is a key element

Cole (2000)

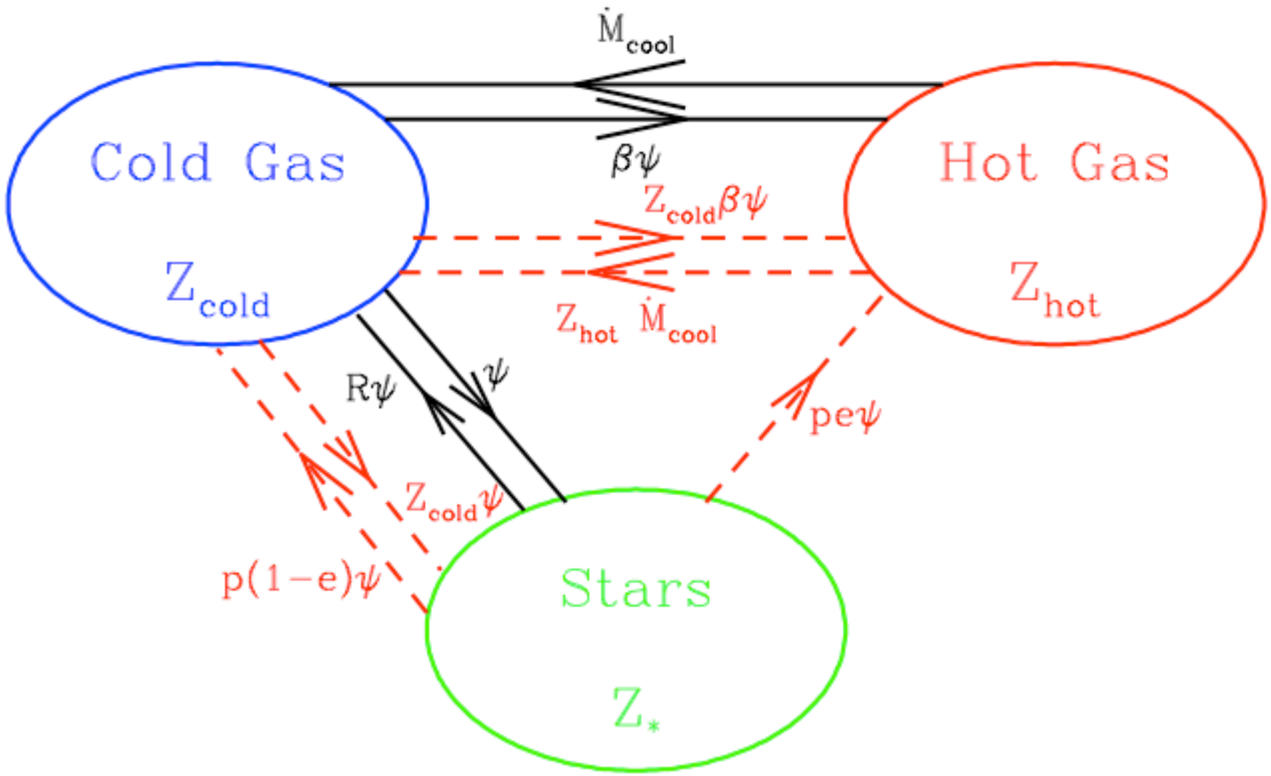

multiple versions of SAMs with slightly different astrophysical processes

Benson (2010)

Table 2: A survey of physical processes included in major semi-analytic models of galaxy formation. In each case we indicate how this process is implemented and give references where relevant. In many cases a single model has implemented a given physical process at different levels of complexity/realism. In such cases, we list the most "advanced" implementation that the model is capable of.

c.f., D. Scott arXiv:1112.0285

	Model				
Feature	DURHAM[1]	MUNICH[2]	SANTA-CRUZ[3]	MORGANA[4]	GALICS[5]
Merger Trees					
→ Analytic	Modified ePS[6]	ePS[7]	ePS	PINOCCHIO[8]	×
→ N-body	✓[9]	✓	✓	×	✓
Halo Profiles	Einasto[10]	Isothermal	NFW	NFW	Empirical[11]
Cooling Model					
→ Metal-dependent	✓	✓	✓	✓	✓
Star Formation	✓	✓	✓	✓	✓
Feedbacks					
→ SNe	✓	✓	✓	✓	✓
→ AGN	✓[12]	✓	✓	✓	✓[13]
→ Reionization	✓[10]	×	✓	✓[14]	✓[15]
Merging					
→ Substructure[16]	N-body[17]	N-body[17]	DF[18]	DF[18]	N-body[17]
→ Substructure–Substructure[19]	✓[20,10]	×	✓[21,22]	×	✓[21]
Environments					
→ Ram Pressure Stripping	✓[23]	✓[24]	×	×	✓[25]
→ Tidal Stripping	✓[10]	×	✓	✓	✓
→ Harassment	×	×	×	×	×
Disks					
→ Disk Stability	✓	✓	✓[26]	✓	✓
→ Dynamical Friction[27]	✓[28]	×	×	×	×
→ Thickness	✓[28]	×	×	×	×
Sizes					
→ Adiabatic contraction	✓	×	✓	✓	×
Chemical Enrichment	✓ [delayed[10]]	✓ [instant[29]]	✓ [delayed[30]]	✓ [instant]	✓ [delayed[31]]
Dust	GRASIL[32]	Screen[33]	Slab[34]	GRASIL[32][35]	Slab[34]

multiple versions of SAMs with slightly different astrophysical processes

Benson (2010)

Notes

[1]Cole et al. (2000);
[2]Croton et al. (2006);
[3]Somerville et al. (2008b);
[4]Monaco et al. (2007);
[5]Hatton et al. (2003);
[6]Parkinson et al. (2008);
[7]Kauffmann and White (1993);
[8]Monaco et al. (2002);
[9]Helly et al. (2003a);
[10]Benson and Bower (2010);
[11]A "dark matter" core is included in calculations of disk sizes with an empirically selected dark matter fraction;
[12]Bower et al. (2006);
[13]Cattaneo et al. (2006);
[14]Macció et al. (2009);
[15]Lanzoni et al. (2005);
[16]How does the model track substructures within halos?;
[17]Substructure orbits and merging times are determined from N-body simulations;
[18]Dynamical Friction: substructure merging times are computed from analytic estimates of dynamical friction timescales
[19]Does the model allow merging between pairs of subhalos orbiting in the same host halo?;
[20]Using hierarchically nested substructures;
[21]Using random collisions of subhalos;
[22]Somerville and Primack (1999);
[23]Font et al. (2008);
[24]Brüggen and Lucia (2008);
[25]Lanzoni et al. (2005);
[26]Somerville et al. (2008a);
[27]Does the model include dynamical friction forces exerted by a galaxy disk on orbiting satellites?;
[28]Benson et al. (2004);
[29]Lucia et al. (2004);
[30]Arrigoni et al. (2009);
[31]Pipino et al. (2008);
[32]Silva et al. (1998);

fundamental issues: uniqueness problem and process complexity

* modeling star formation in direct gas dynamic simulations requires
  - correct modeling of shocks
  - correct cooling in a plasma heated by multiple processes (non-LTE?)
  - modeling of magnetic fields + cosmic ray heating?
  - detailed mass loading and metal pollution by SN blastwaves
  - detailed effects of jet heating from central BH (AGN activity)
  - +...

  All of this requires many tens of input parameters, effects of which often compete against one another. How do we know when we've reached THE solution of nature? Does nature even follow a unique prescriptive solution? Or might elements be stochastic?

  Also, star formation, including the stellar IMF and feedback processes, are assumed to be dependent only on local conditions, independent of time. Is this really correct?

* SAM models already have >100 input parameters...

Will we ever declare galaxy formation a \`solved problem’?

end run: ***statistical*** solutions for galaxy formation

Zehavi etal (2010)

* Halo Occupation Distribution (HOD) method:
assign galaxies to halos

– for given minimum luminosity, know n(L,z) empirically
– also know n(M,z) from sims
– also know two-point clustering of halos and galaxies
– write $p(N_{gal} \mid M,z)$ to match n(L,z) and clustering

Conroy etal (2006)

* Sub-Halo Assignment Matching (SHAM) method:
assign galaxies to sub-halos

– for given minimum luminosity, know n(L,z) empirically
– also know n(M,z) and $n(M_{sub}, z)$ from sims
– within given volume, rank order L and M_{sub}, and match ranks to assign L to M_{sub}
– scatter can be introduced during ranking process

SDSS counts and clustering constraints on the Halo Occupation Distribution

Zehavi et al. 2010

$$\langle N(M_h)\rangle = \frac{1}{2}\left[1+\mathrm{erf}\left(\frac{\log M_h - \log M_{\min}}{\sigma_{\log M}}\right)\right]\left[1+\left(\frac{M_h - M_0}{M_1'}\right)^{\alpha}\right], \tag{6}$$

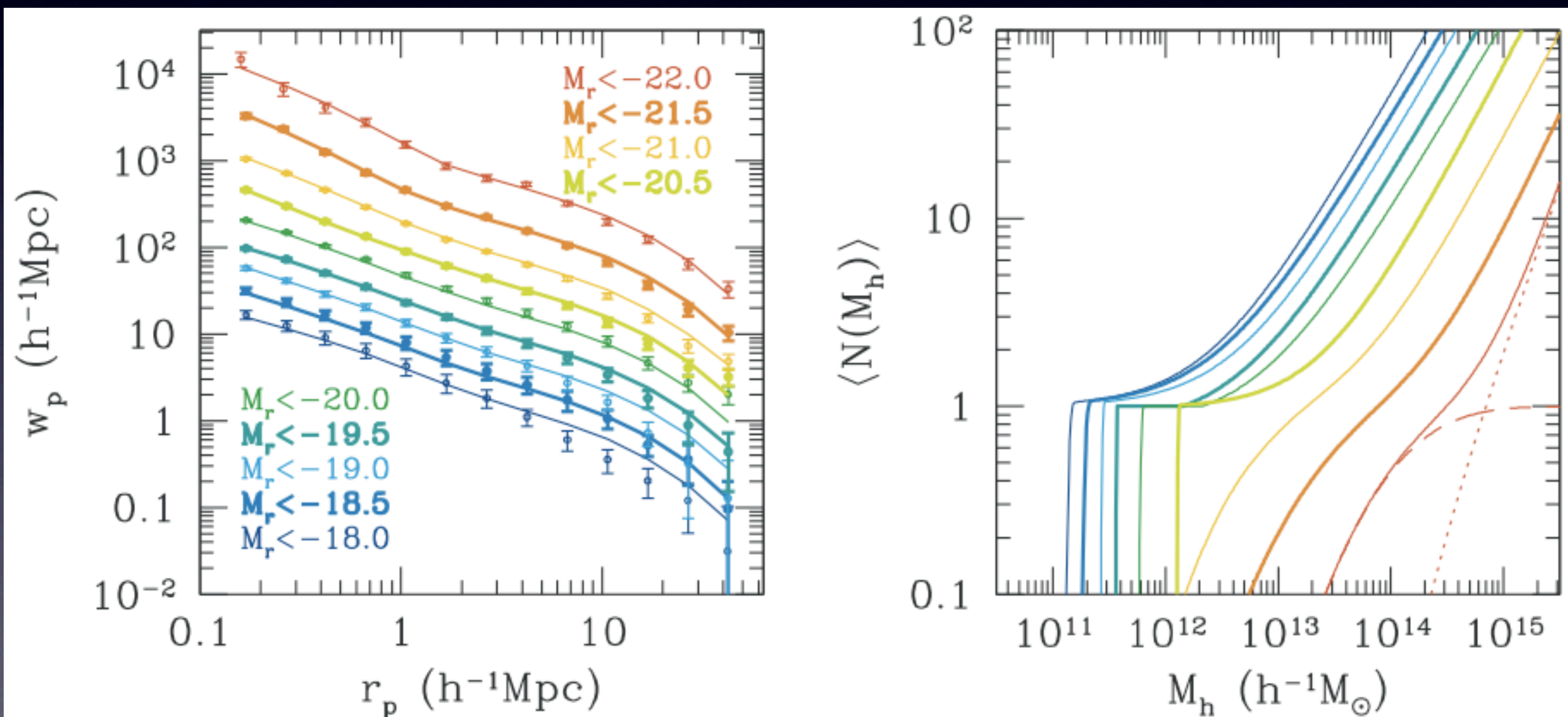

SDSS counts and clustering constraints on the Halo Occupation Distribution

Zehavi et al. 2010

TABLE 3
HOD AND DERIVED PARAMETERS FOR LUMINOSITY THRESHOLD SAMPLES

M_r^{max}	$\log M_{min}$	$\sigma_{\log M}$	$\log M_0$	$\log M_1'$	α	$\log M_1$	b_g	f_{sat}	χ^2/dof
-22.0	14.06 ± 0.06	0.71 ± 0.07	13.72 ± 0.53	14.80 ± 0.08	1.35 ± 0.49	14.85 ± 0.04	2.16 ± 0.05	0.043 ± 0.003	1.8
-21.5	13.38 ± 0.07	0.69 ± 0.08	13.35 ± 0.21	14.20 ± 0.07	1.09 ± 0.17	14.29 ± 0.04	1.67 ± 0.03	0.094 ± 0.004	2.3
-21.0	12.78 ± 0.10	0.68 ± 0.15	12.71 ± 0.26	13.76 ± 0.05	1.15 ± 0.06	13.80 ± 0.03	1.40 ± 0.03	0.146 ± 0.007	3.1
-20.5	12.14 ± 0.03	0.17 ± 0.15	11.62 ± 0.72	13.43 ± 0.04	1.15 ± 0.03	13.44 ± 0.03	1.29 ± 0.01	0.204 ± 0.009	2.7
-20.0	11.83 ± 0.03	0.25 ± 0.11	12.35 ± 0.24	12.98 ± 0.07	1.00 ± 0.05	13.08 ± 0.03	1.20 ± 0.01	0.218 ± 0.012	2.1
-19.5	11.57 ± 0.04	0.17 ± 0.13	12.23 ± 0.17	12.75 ± 0.07	0.99 ± 0.04	12.87 ± 0.03	1.14 ± 0.01	0.229 ± 0.010	1.0
-19.0	11.45 ± 0.04	0.19 ± 0.13	9.77 ± 1.41	12.63 ± 0.04	1.02 ± 0.02	12.64 ± 0.04	1.12 ± 0.01	0.332 ± 0.014	1.8
-18.5	11.33 ± 0.07	0.26 ± 0.21	8.99 ± 1.33	12.50 ± 0.04	1.02 ± 0.03	12.51 ± 0.04	1.09 ± 0.01	0.339 ± 0.015	0.9
-18.0	11.18 ± 0.04	0.19 ± 0.17	9.81 ± 0.62	12.42 ± 0.05	1.04 ± 0.04	12.43 ± 0.05	1.07 ± 0.01	0.320 ± 0.022	1.4

NOTE. — See § 2.3 for the HOD parameterization. Halo mass is in units of $h^{-1}M_\odot$. Error bars on the HOD parameters correspond to 1σ, derived from the marginalized distributions. M_1, b_g and f_{sat} are derived parameters from the fits; M_1 is the mass scale of a halo that can on average host one satellite galaxy above the luminosity threshold, b_g is the large-scale galaxy bias factor, and f_{sat} is the fraction of satellite galaxies in the sample. For all samples, the number of degrees-of-freedom (dof) is 9 (13 measured w_p values plus the number density minus the five fitted parameters).

significant scatter in minimum mass needed to house bright galaxies - what is this telling us?

slope of satellite number is very close to one

one percent errors on bias measurement!

SDSS counts and clustering constraints on the Halo Occupation Distribution

Zehavi et al. 2010

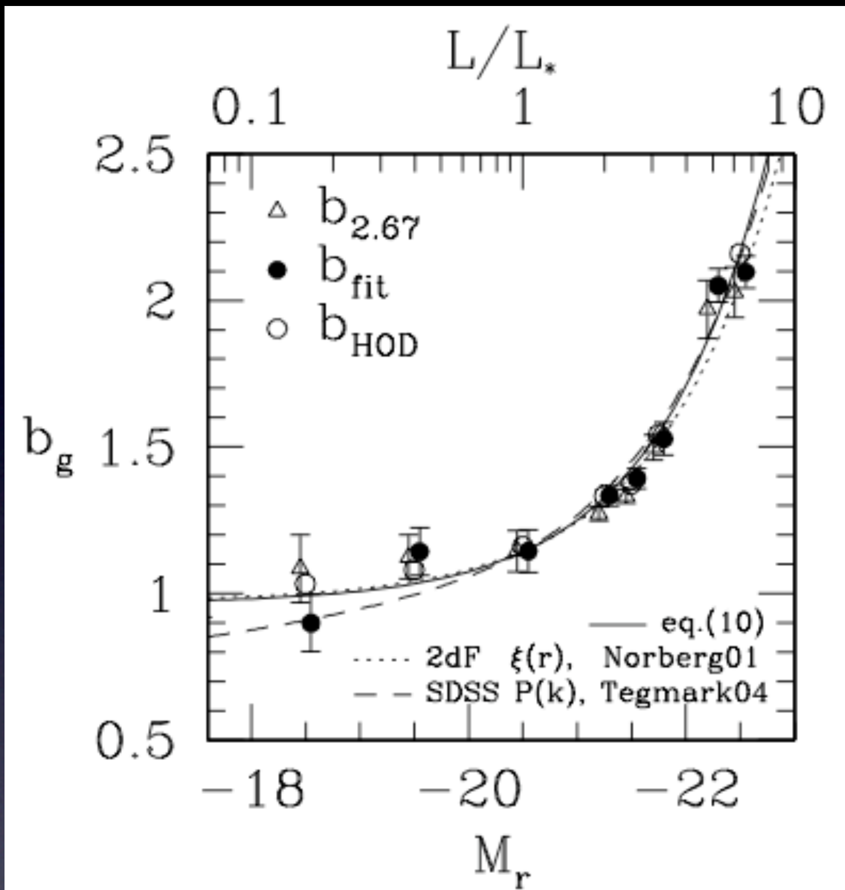

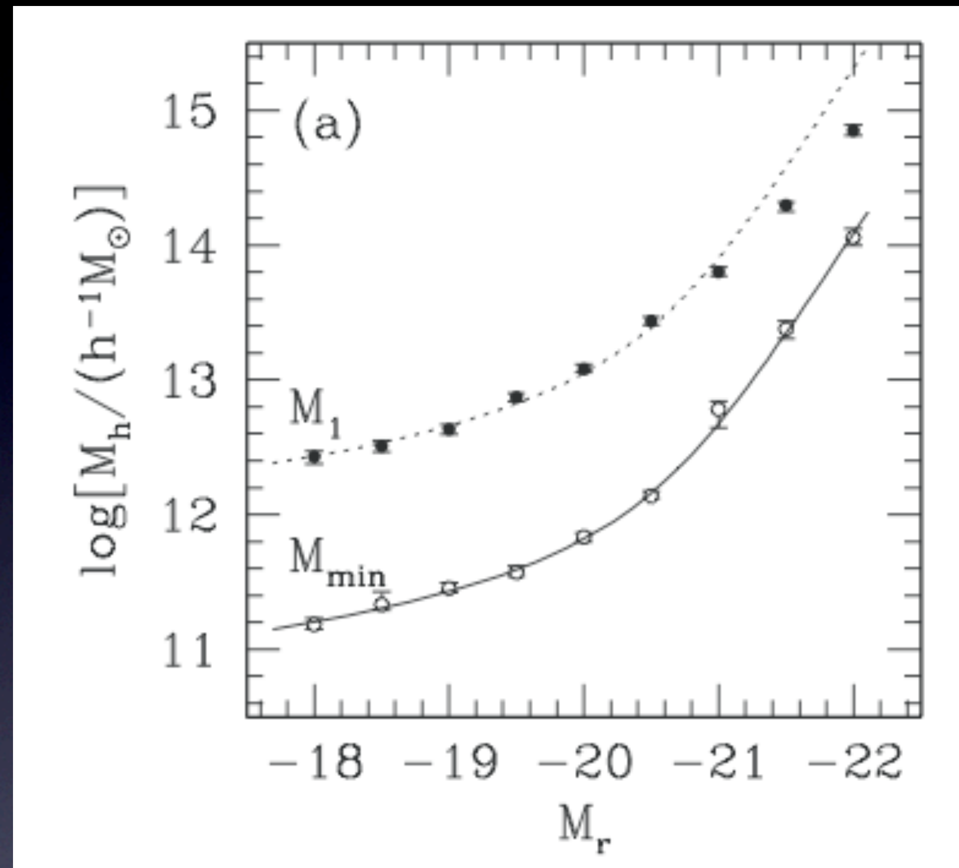

passive (red) galaxies dominate SDSS groups and clusters

Balogh & McGee 2010

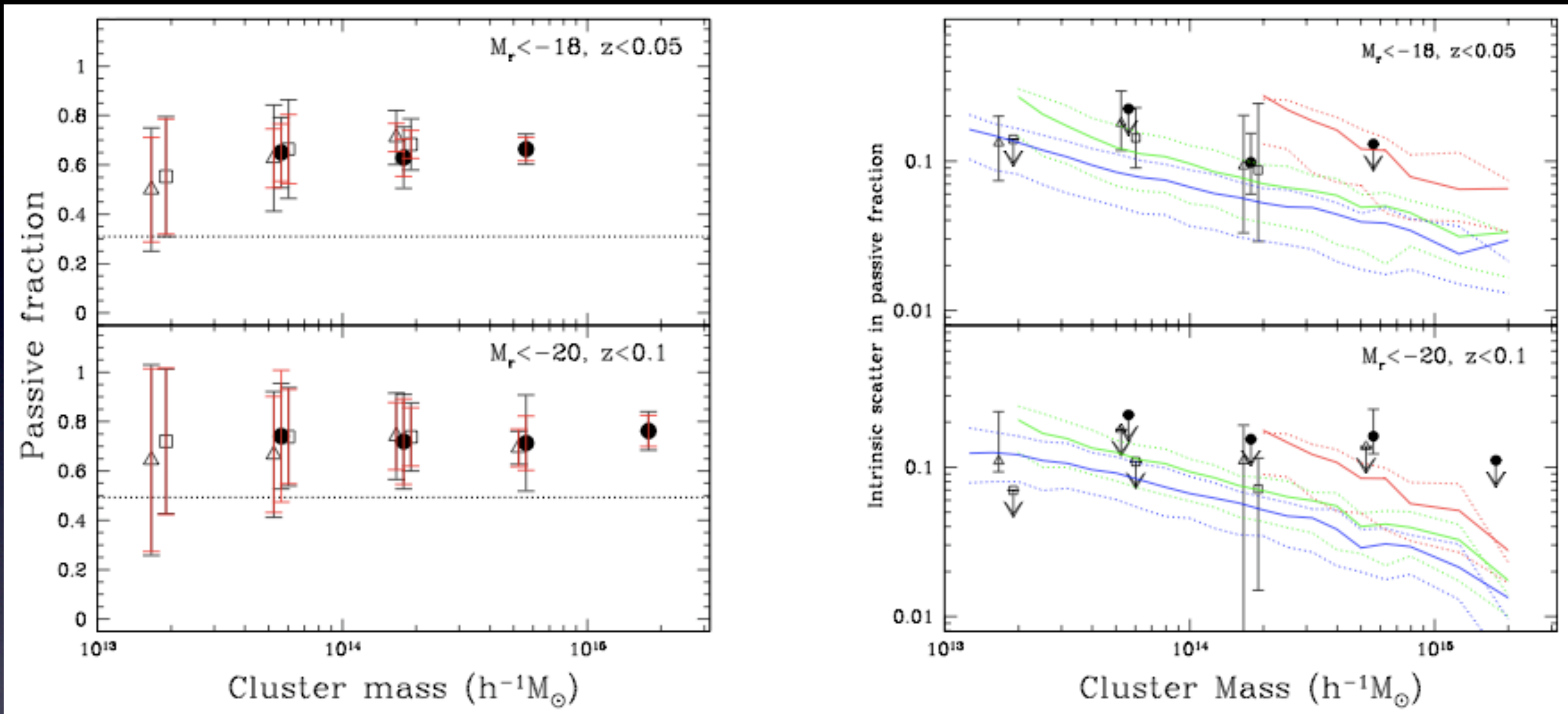

SDSS DR6 analysis
3 different group/cluster catalogs:
- 2 optical (Yang (2005) + Berlind (2006)
- 1 X-ray (HIFLUGCS, Reiprich + Boehringer 2002)

passive = red in *r–i* and *u–g* colors

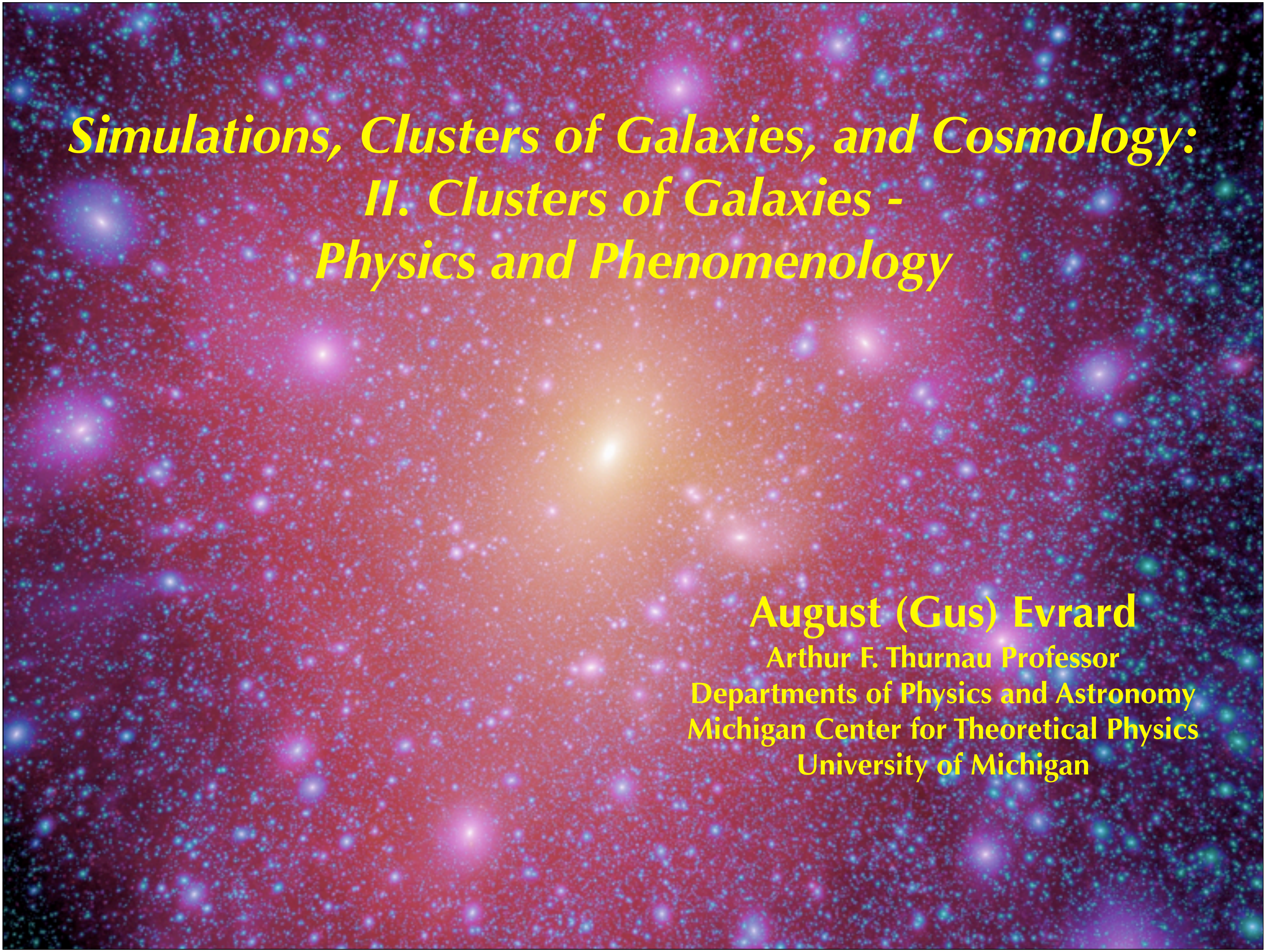

Simulations, Clusters of Galaxies, and Cosmology: II. Clusters of Galaxies - Physics and Phenomenology

August (Gus) Evrard
Arthur F. Thurnau Professor
Departments of Physics and Astronomy
Michigan Center for Theoretical Physics
University of Michigan

moving up the hierarchy to model clusters of galaxies

* observations indicate that baryons in M>1e14 Msun halos are mainly in a hot, intracluster medium (ICM)
  - hot gas outweighs baryons in stars by factors >~5
  - zero-eth order treatment: ignore galaxy formation entirely (gravity + shock heating)
  - first-order treatment: include heating effects of galaxy formation on ICM via a `preheated' assumption => elevate gas entropy at high z

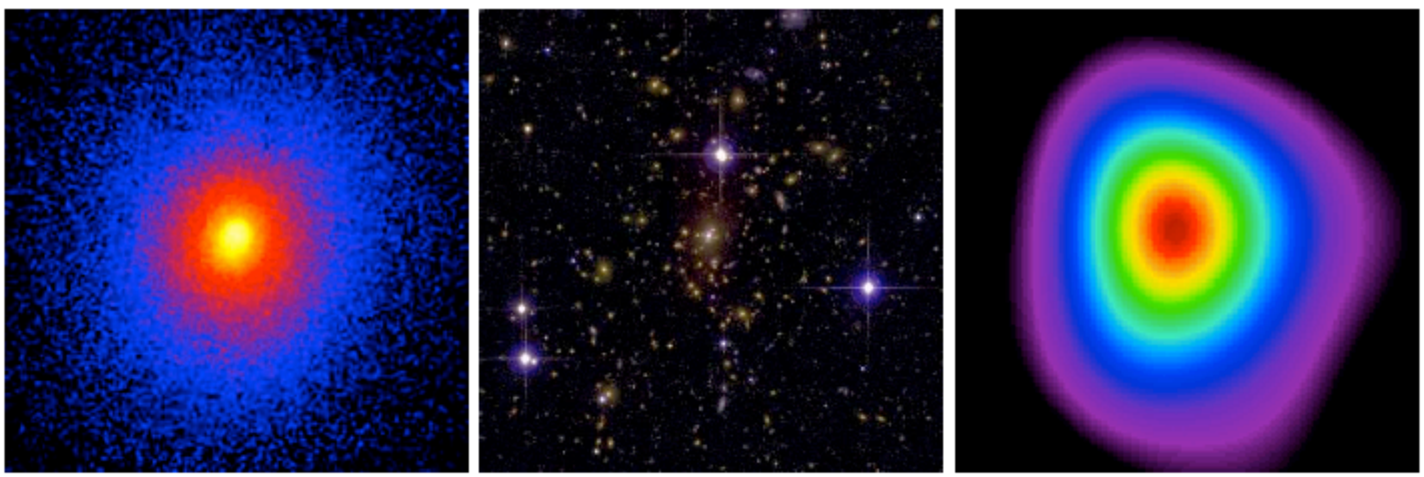

Figure 7: Images of Abell 1835 ($z = 0.25$) at X-ray, optical and mm wavelengths, exemplifying the regular multi-wavelength morphology of a massive, dynamically relaxed cluster. All three images are centered on the X-ray peak position and have the same spatial scale, 5.2 arcmin or ~ 1.2 Mpc on a side (extending out to $\sim r_{2500}$; Mantz et al. 2010a). Figure credits: *Left*: X-ray: Chandra X-ray Observatory/A. Mantz; *Center*, Optical: Canada France Hawaii Telescope/A. von der Linden et al.; *Right*, SZ: Sunyaev Zel'dovich Array/D. Marrone.

Millennium Gas Simulations

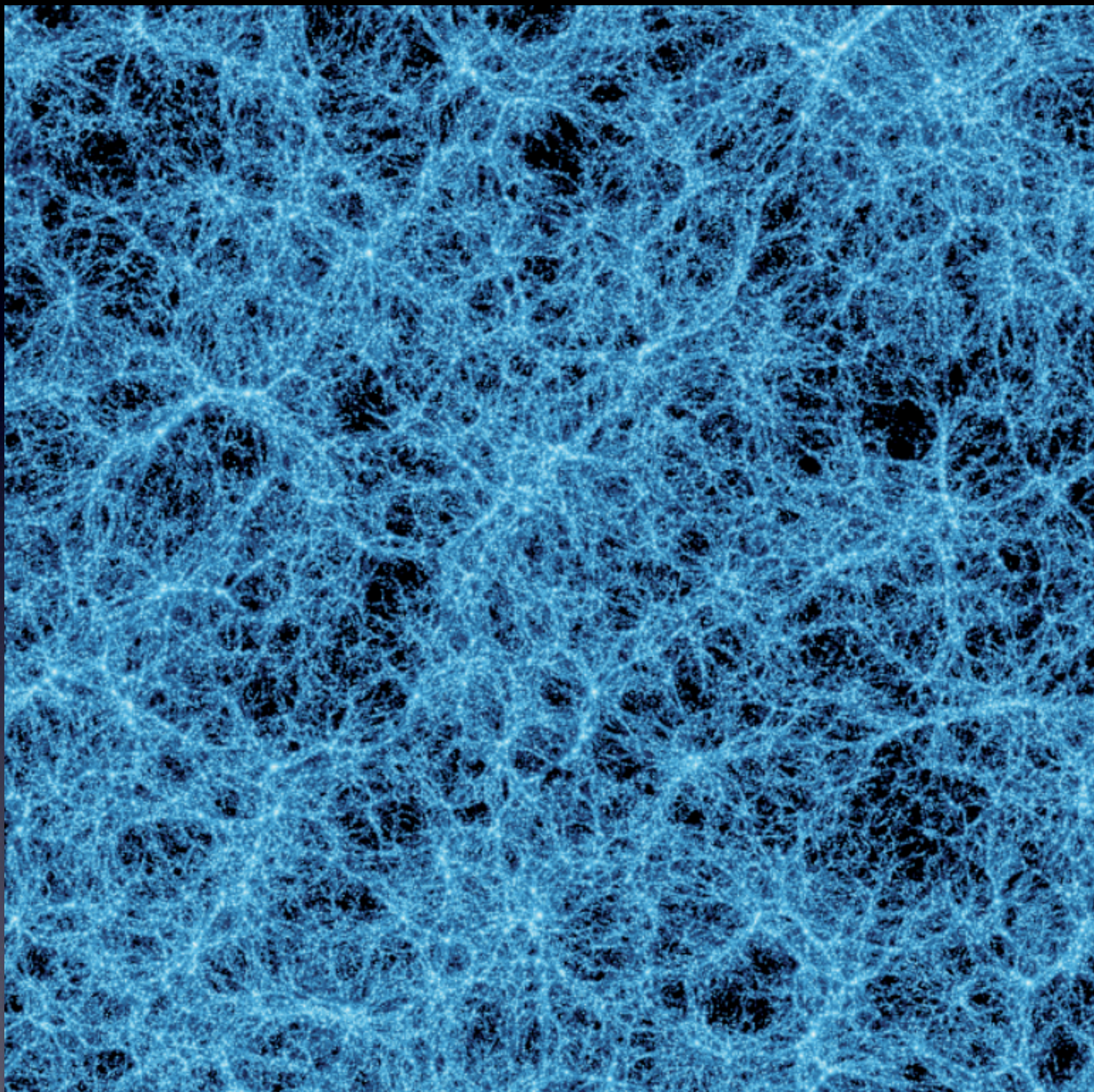

GADGET-2 resimulations of Millennium Sim volume @ Nottingham (F. Pearce)

- 500 Mpc/h
- 1e9 gas+DM particles
- m_p(DM) ~ 1.4e10 Msun
- 25 kpc/h softening
- same cosmology as MS

TWO physical treatments:

GO: gravity only

PH: preheated gas
200 keV-cm2 @z=4

Hartley et al. (2008)
Stanek, Rudd, AE (2009)
Stanek et al., 0910.1599
Short et al., 1002.4539

brief history of preheating...

- introduced in back-to-back ApJ papers almost 20 years ago to solve n(Lx) shape for `standard' CDM model

Kaiser (1991)
Evrard & Henry (1991)

- simulations tuned entropy level required to `tilt' L-T relation to match observations

Bialek et al (2001)

- motivated by predominance of `red + dead' galaxies in rich clusters => formed stars and SMBH at early epoch
- empirical support from Chandra analysis of core entropy behavior (ACCEPT sample)

Cavagnolo et al (2009)

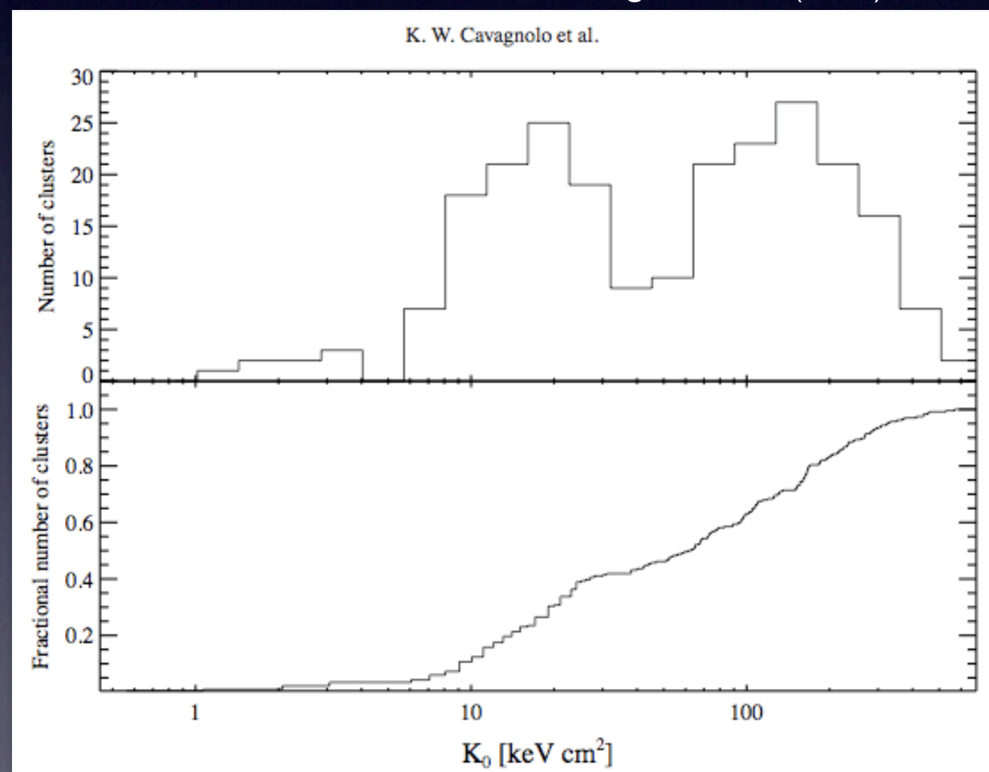

MGS massive halo yield

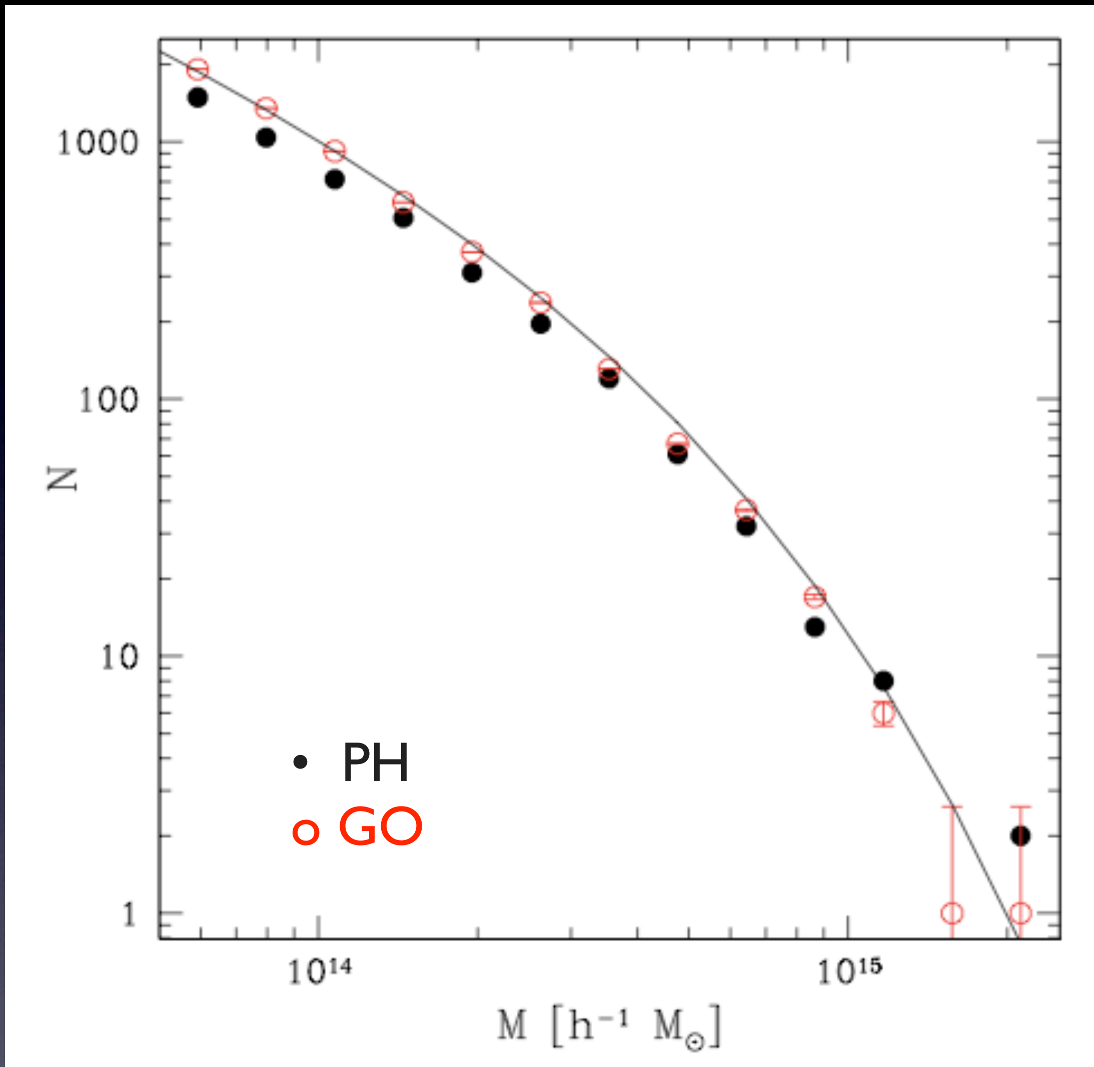

– halos at z=0 with $M_{200c} \geq$ 5e13 Msun/h:

4474 (PH)
5612 (GO)

– 63 output redshifts to z=2 for population evolution, halo formation histories

>100,000 halos overall

MGS scaling : mass-weighted temperature

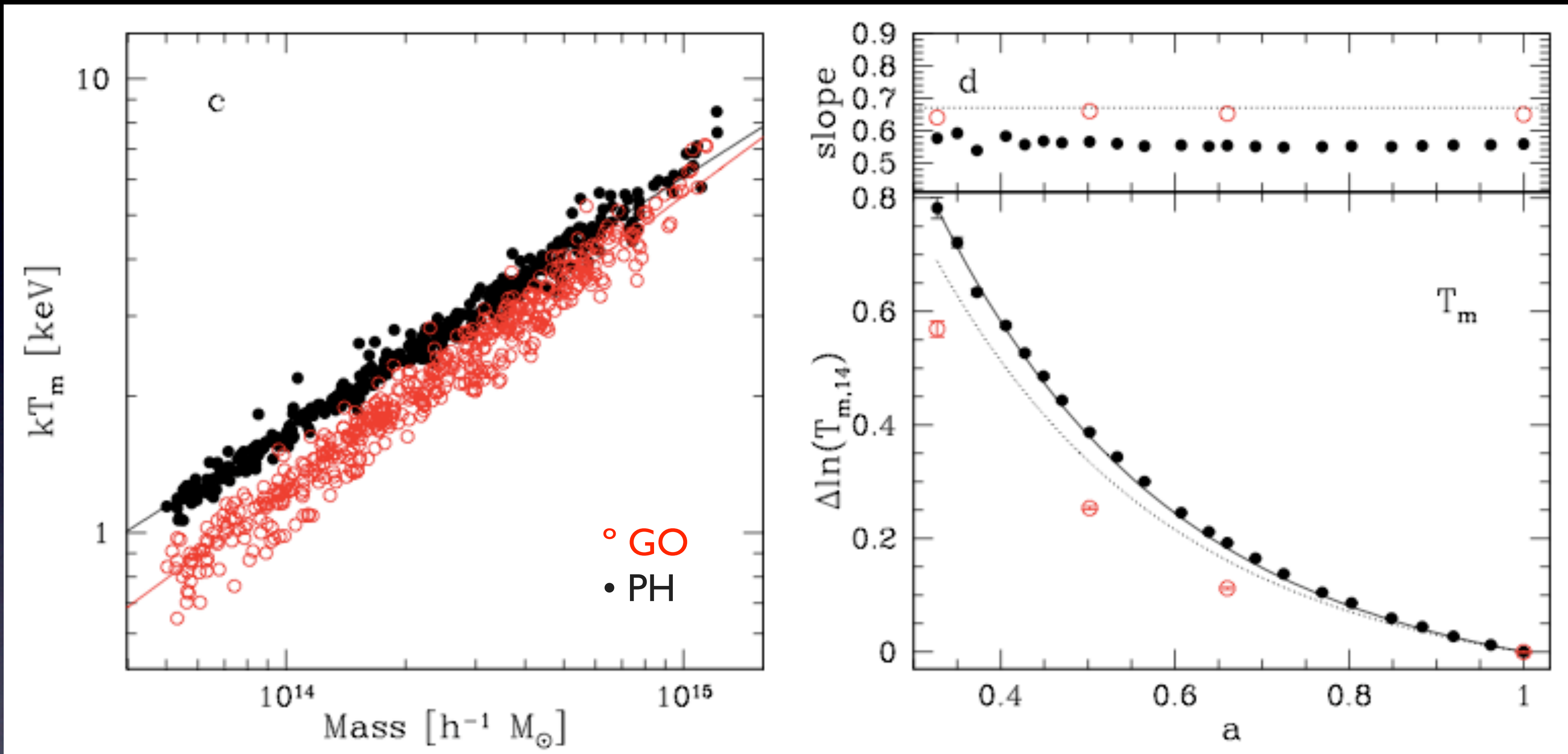

mass scaling at z=0
(random subsample
~uniform in mass)
solid: power-law fit

evolution of slope and
intercept at 10^14 Msun/h
solid: E(a)^alpha fit
dashed: self-similar expectation

MGS scaling : ICM mass fraction

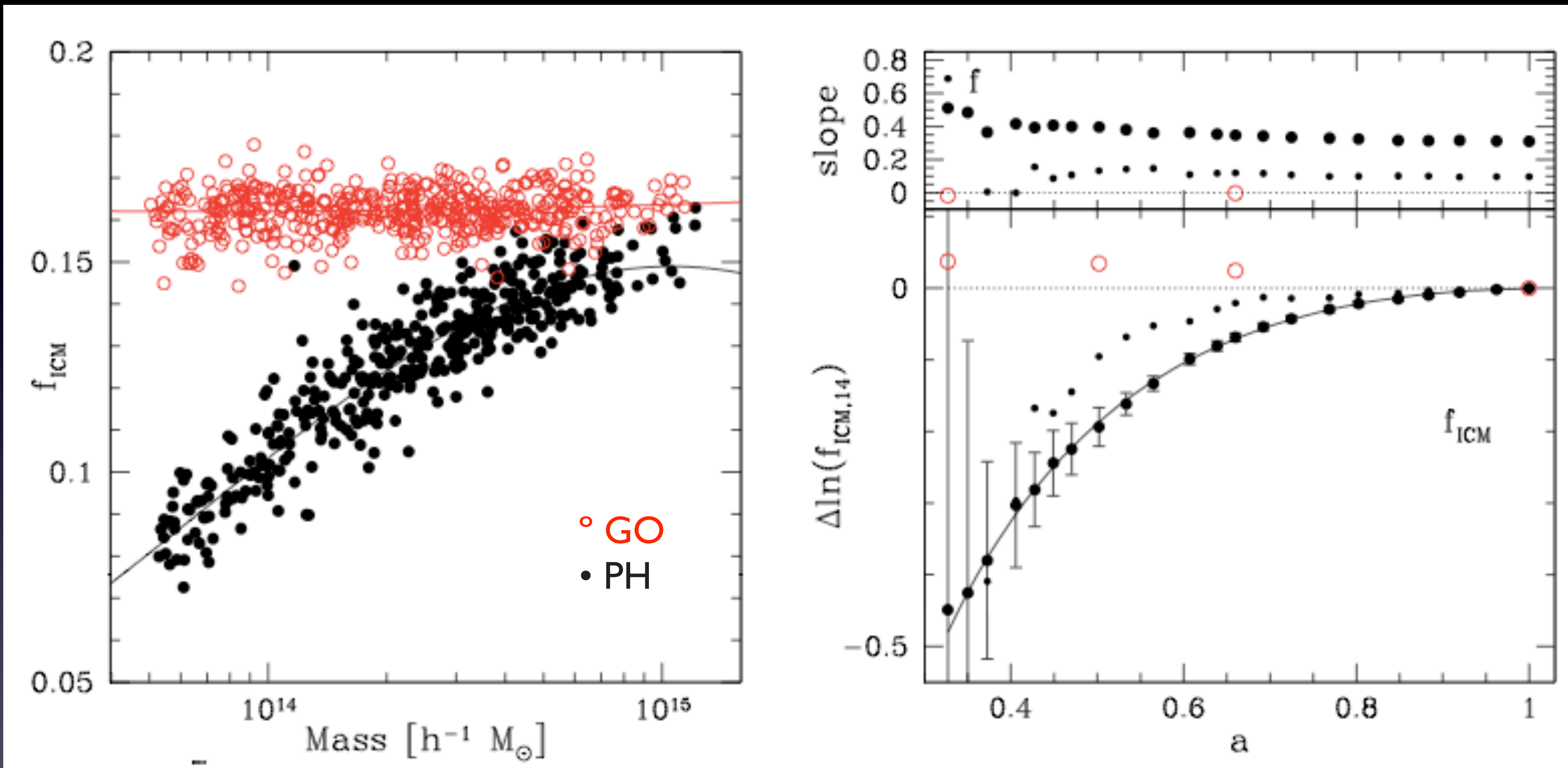

solid: quadratic fit in ln(M)

large dots: values at 1e14 Msun/h
small dots: values at 5e14 Msun/h

MGS scaling : SZ Y-parameter (gas thermal energy)

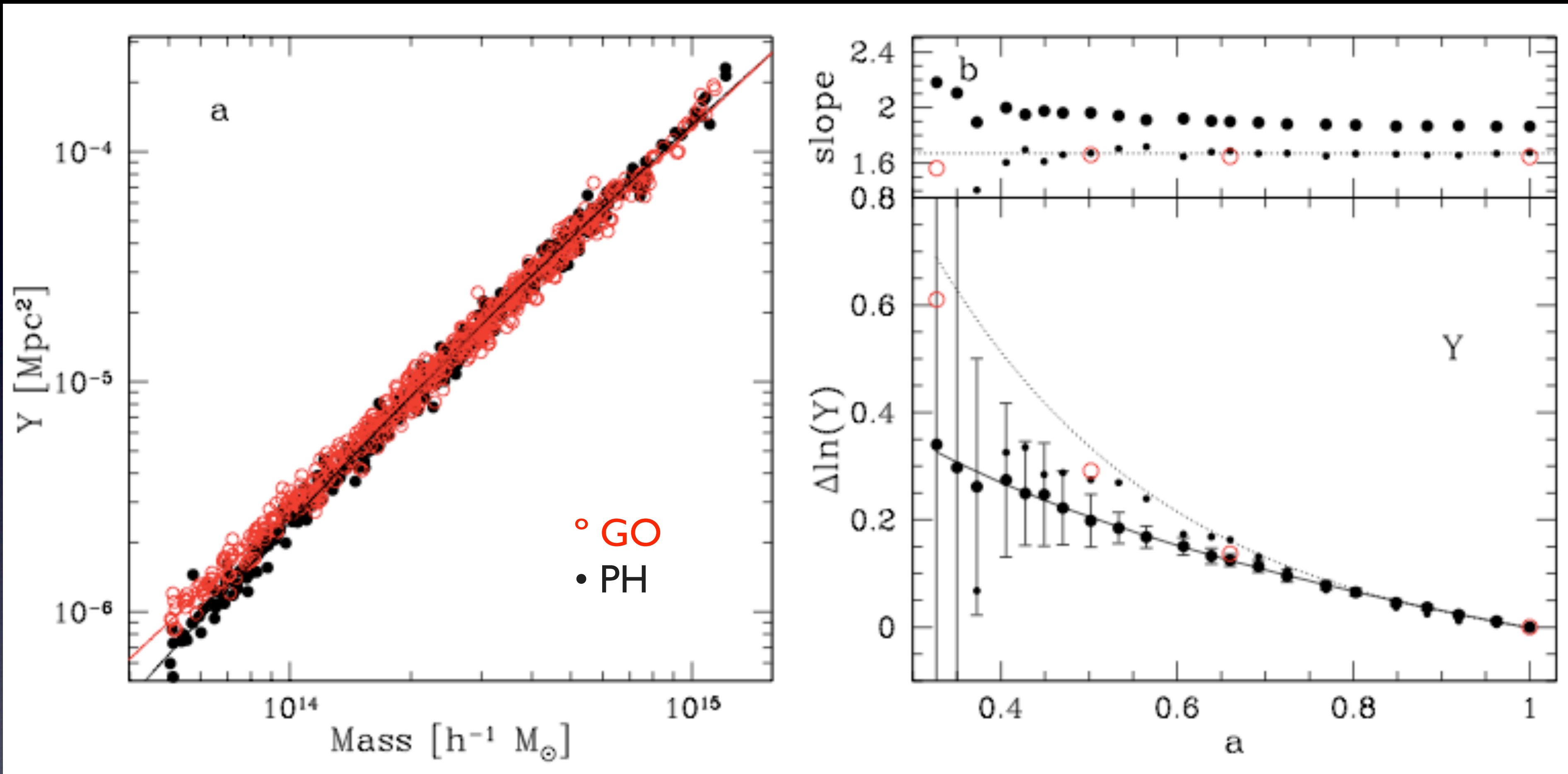

solid: quadratic fit in ln(M)

large dots: values at 1e14 Msun/h
small dots: values at 5e14 Msun/h
solid: quadratic fit in ln(a)

MGS scaling : bolometric X-ray luminosity

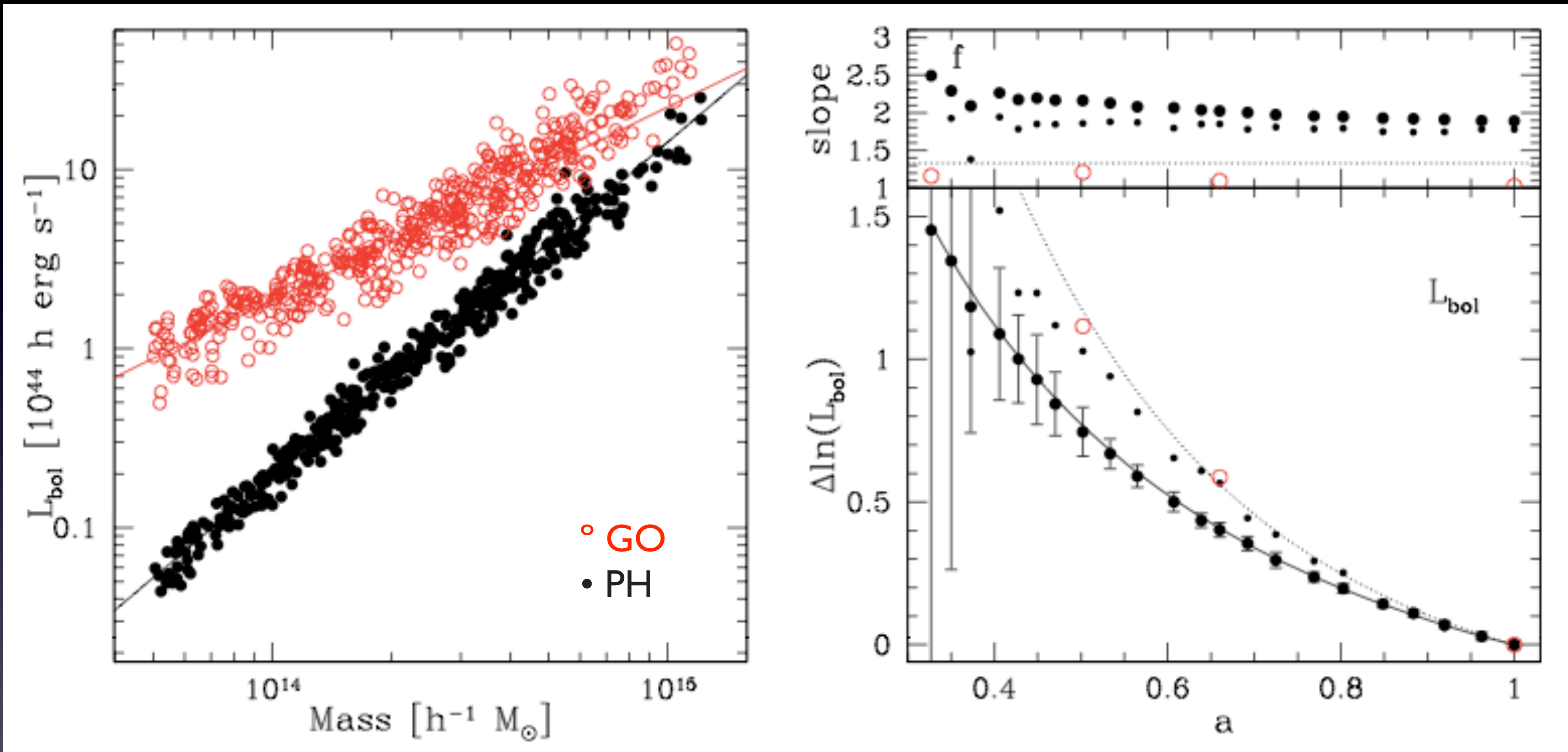

solid: quadratic fit in ln(M)

large dots: values at 1e14 Msun/h
small dots: values at 5e14 Msun/h
solid: quadratic fit in ln(a)

covariance of multiple signals at fixed halo mass

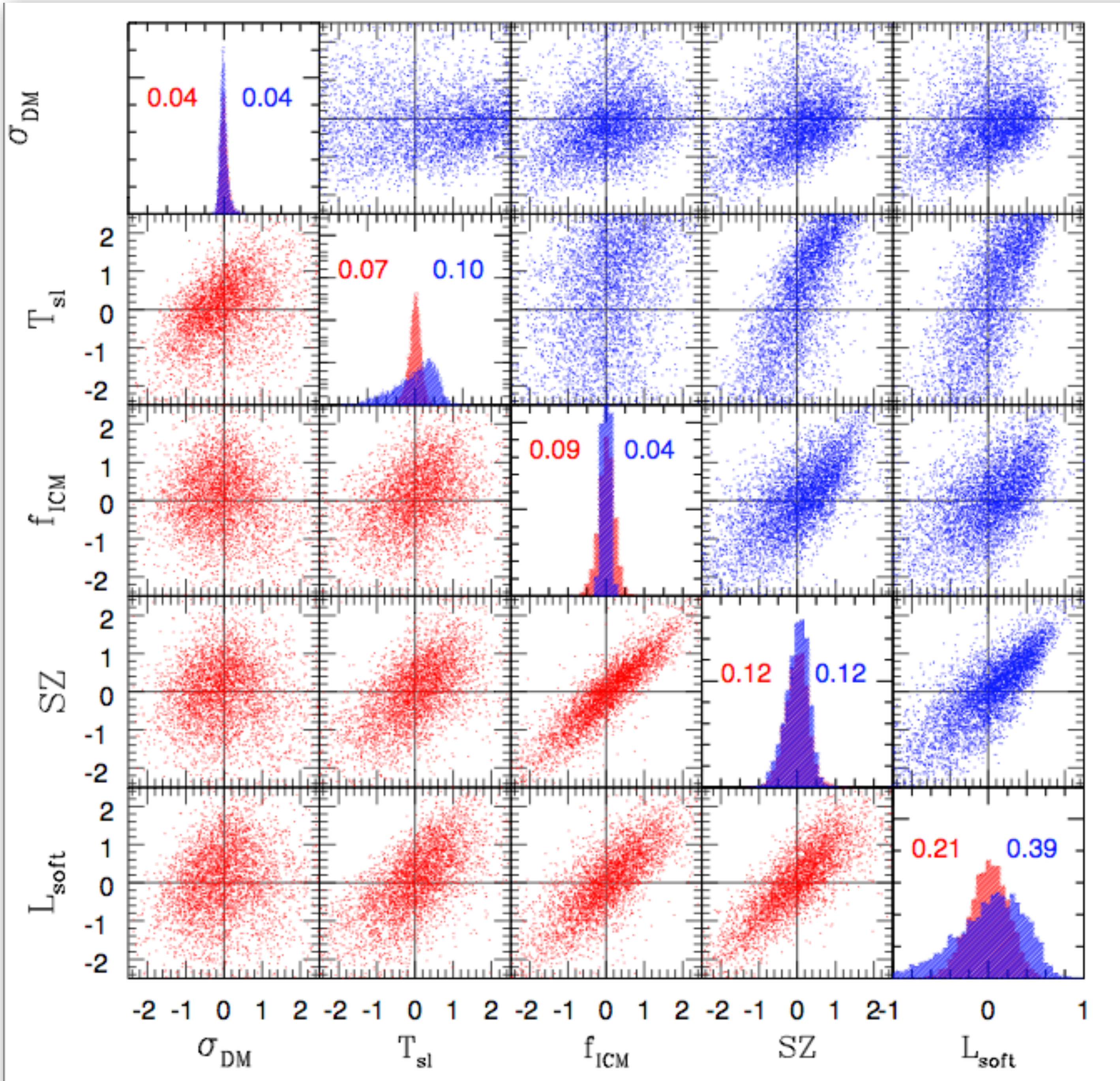

Stanek et al, 2010

preheating
gravity only

synthetic XMM images of Millennium Preheat cluster simulations

Rasia et al, in prep.

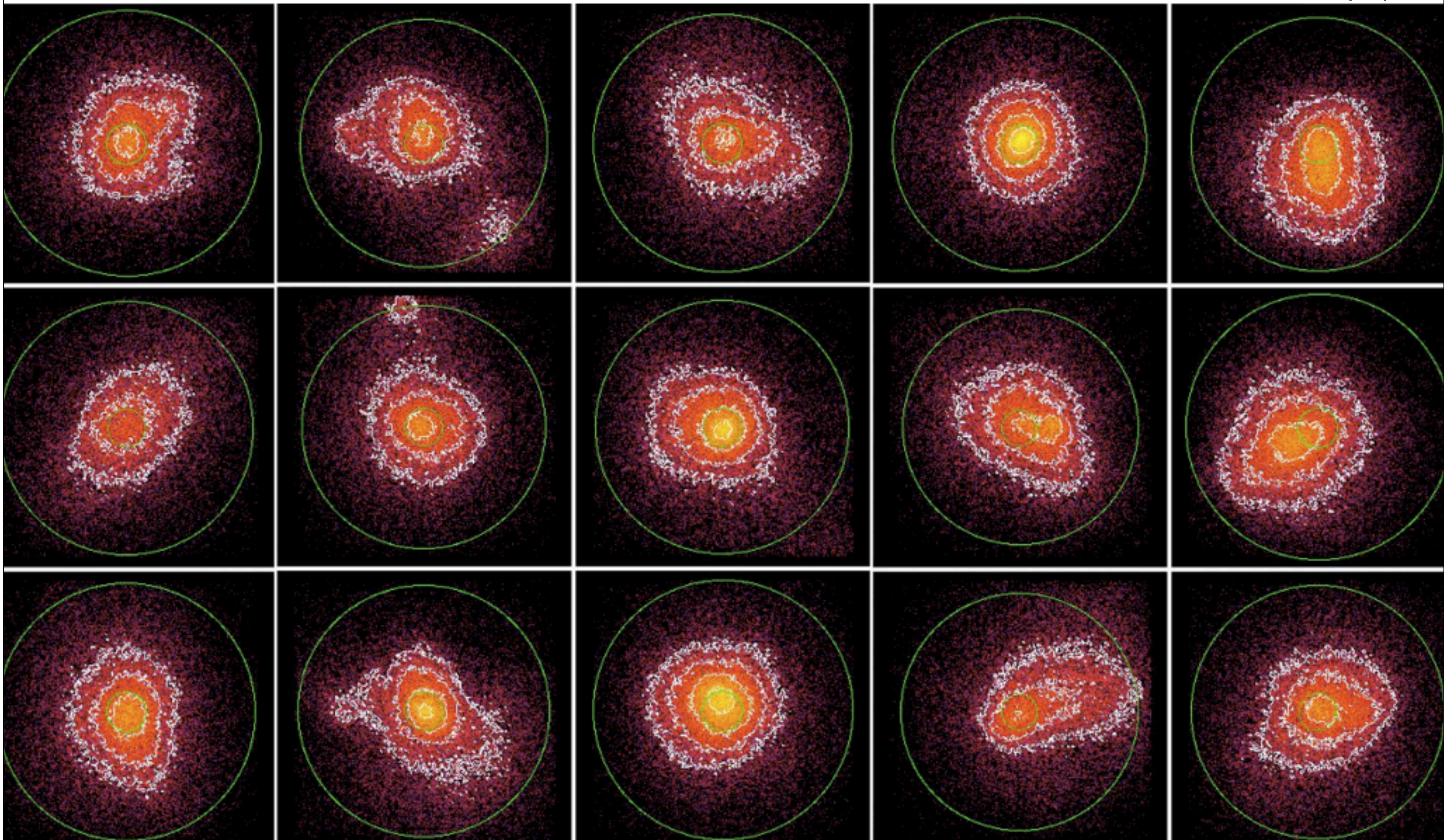

XMM images of REXCESS cluster sample

Pratt et al (2008)

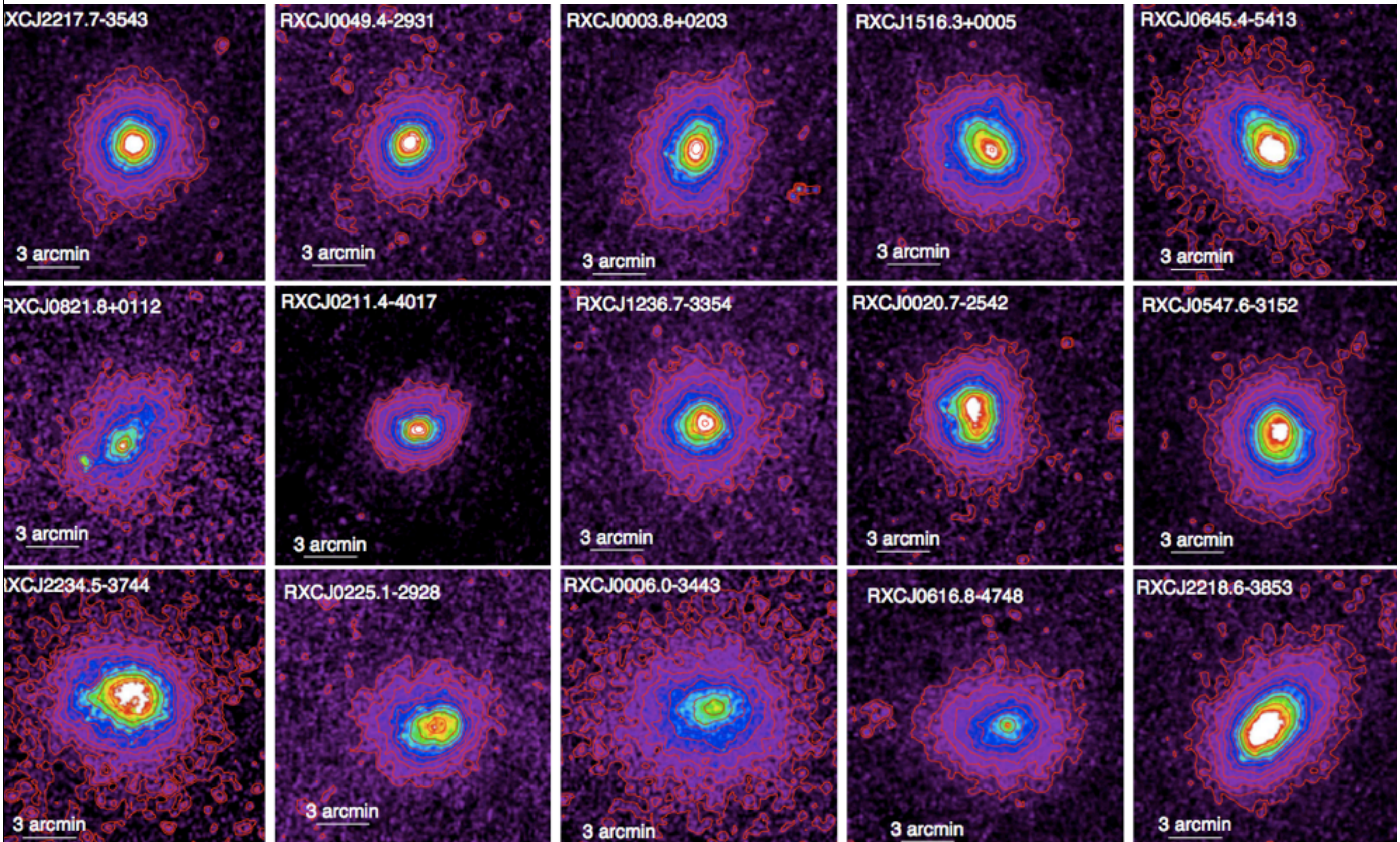

halo scaling laws from Millennium Simulation with gas dynamics treatments

Stanek et al (2010)

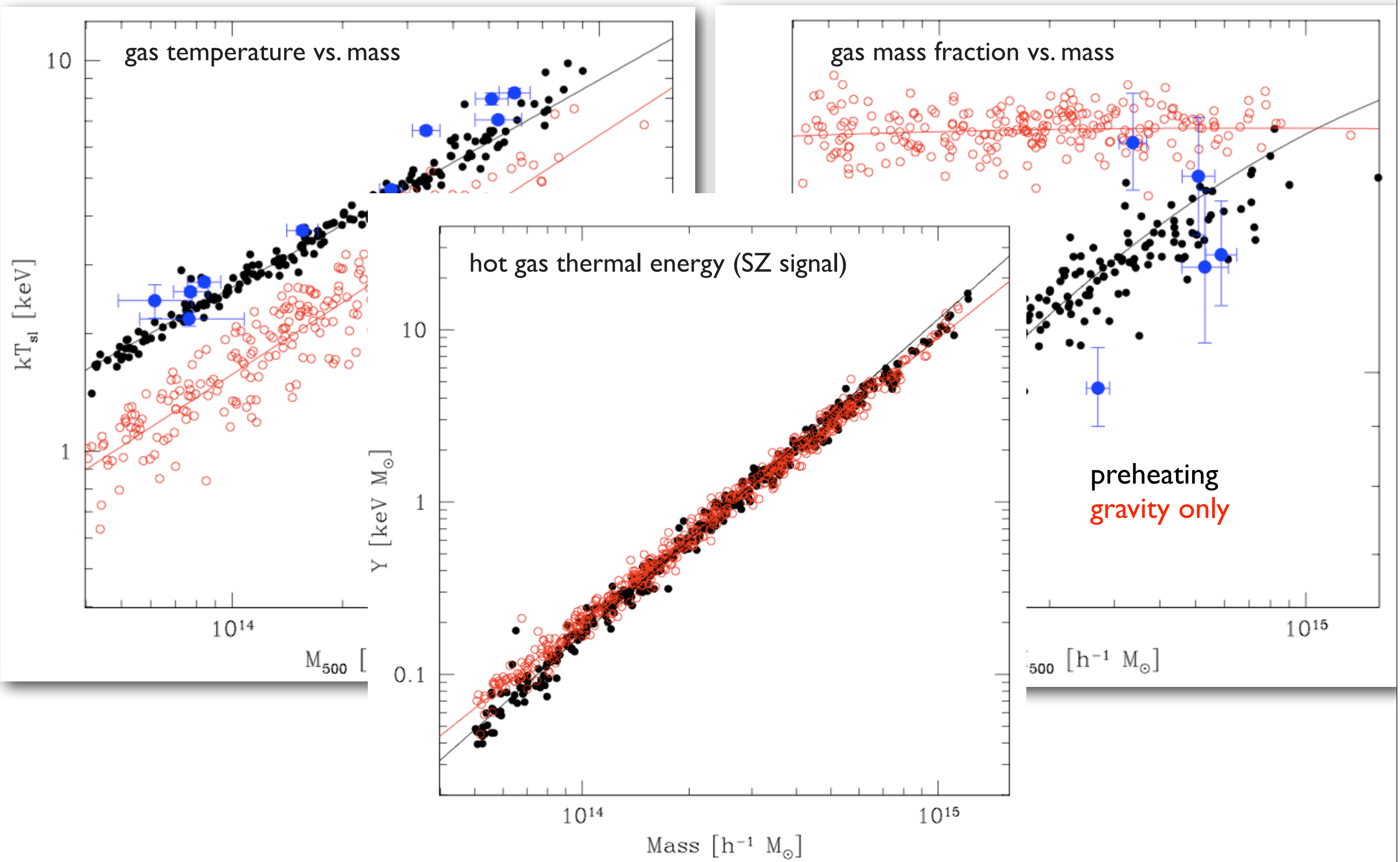

toward cosmology with clusters
(more this afternoon)

physical processes in massive halos and cluster phenomenology

* shock heating
- thermalizes kinetic energy of mergers
- accelerates non-thermal electrons
  => radio synchrotron
- thermal electrons inverse Compton scatter CMB => Sunyaev-Zel'dovich (SZ) effect

* (weak) radiative cooling
- bremsstrahlung+line emission from ICM
  => X-ray emission at kT~1-10 keV

* core processes ~ ISM galactic physics
- heating from central AGN?
- MHD marginal instabilities?

van Weeren et al. (2010)

CIZA J2242.8+5301 (z = 0.1921)

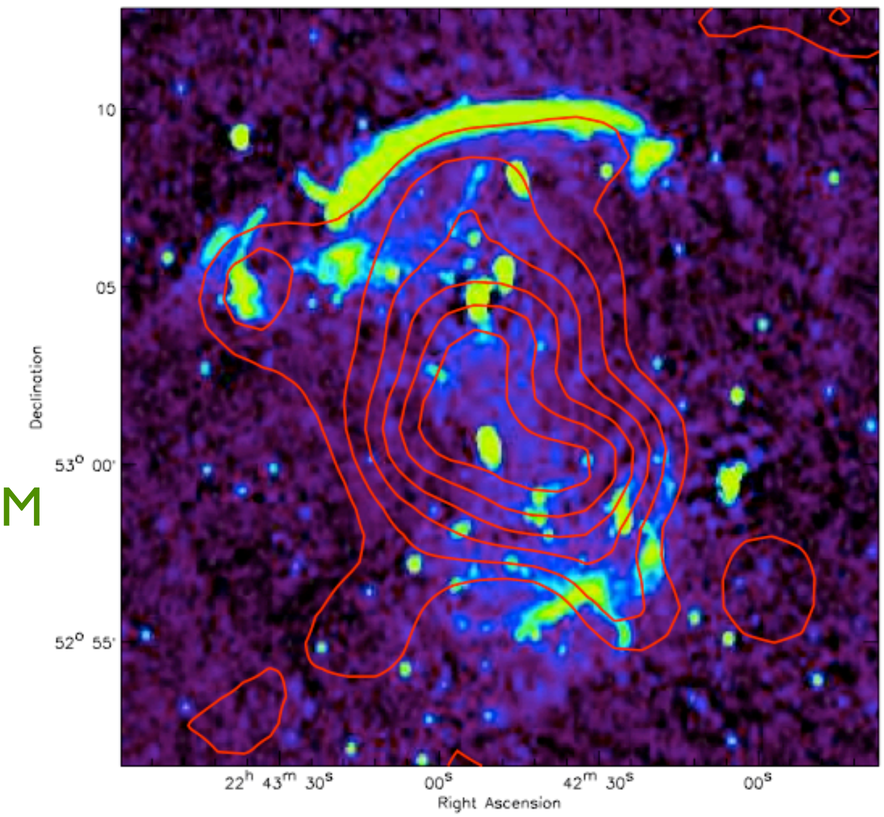

Figure 1: WSRT radio image at 1.4 GHz. The image has a resolution of 16.5 arcsec × 12.9 arcsec and the rms noise is 19 μJy beam^{-1}. Red contours (linearly spaced) represent the X-ray emission from ROSAT showing the hot ICM.

* AGN jets can blow significant bubbes in ICM
  - how frequent is this activity?
  - how is the bubble energy thermalized?

McNamara + Nulsen (2007) ARAA

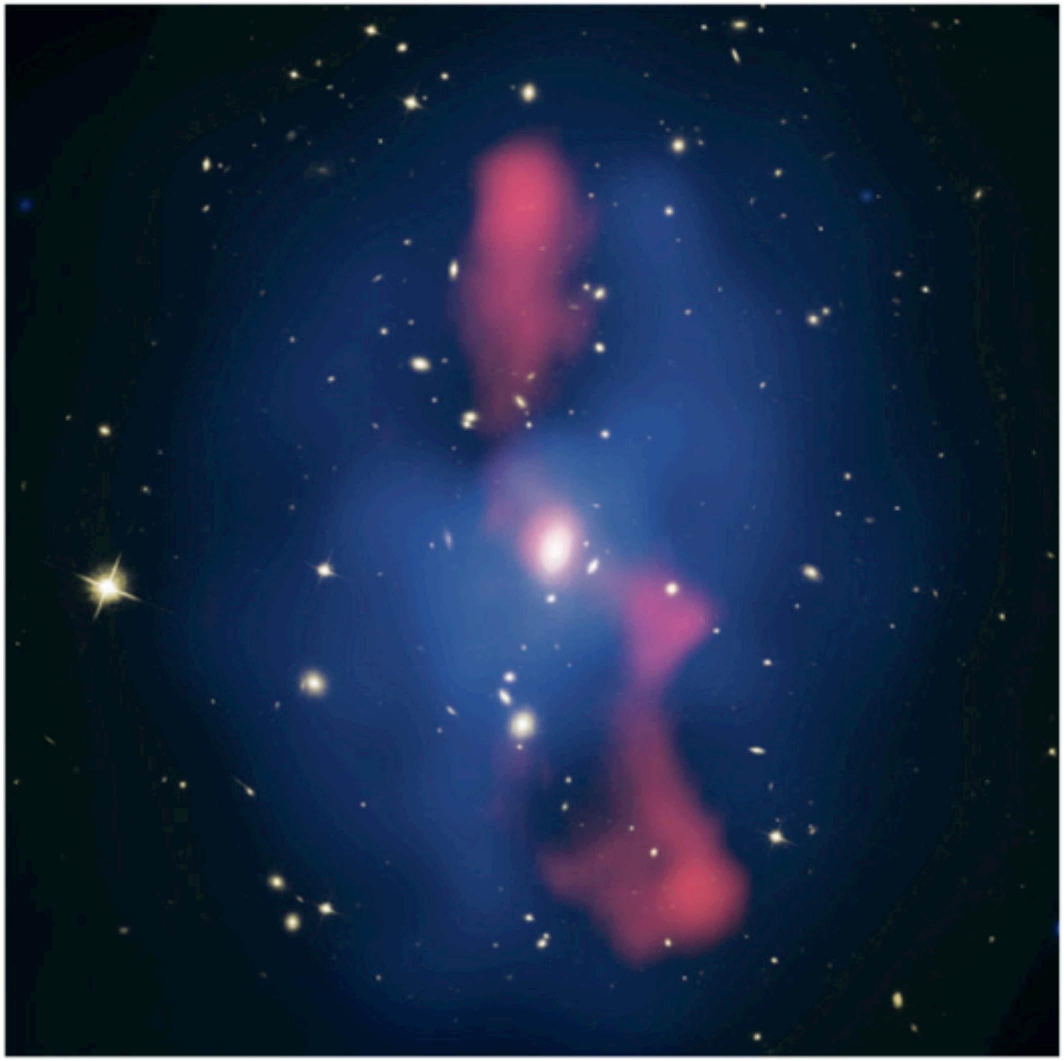

Figure 2

Hubble Space Telescope visual image of the MS0735.6+7421 cluster superposed with the *Chandra* X-ray image in blue and a radio image from the Very Large Array at a frequency of 330 MHz in red. The X-ray image shows an enormous pair of cavities, each roughly 200 kpc in diameter that are filled with radio emission. The radio jets have been inflating the cavities for 10^8 years with an average power of $<2 \times 10^{46}$ erg s^{-1}. The displaced gas mass is $<10^{12}$ $M_\odot$. The cavities and radio source are bounded by a weak shock front. The cavities are well outside the central galaxy and cooling region of the cluster. The supermassive black hole grew by at least $<3 \times 10^8$ $M_\odot$ during the outburst.

what are clusters of galaxies? Perspectives from different communities

to a ***theorist/modeler***

huge, **quasi-equilibrium dark matter clumps** (***halos***) formed at high peaks in the matter density field (on ~10 Mpc scales)

to an ***optical observer***

ahem!... bound **assemblages of galaxies**!

to an ***X-ray observer***

sources of **diffuse X-ray emission** from a hot, metal-enriched plasma

to a ***sub-mm/radio observer***

sources of **spectral distortion** in the microwave background radiation

to ***all observers***

sources of **high magnification** of the light from distant objects

(i.e., *the* largest telescopes in our universe!)

clusters are found at low and high redshift as red galaxy concentrations

Koester et al (2007)

Eisenhardt et al (2008)

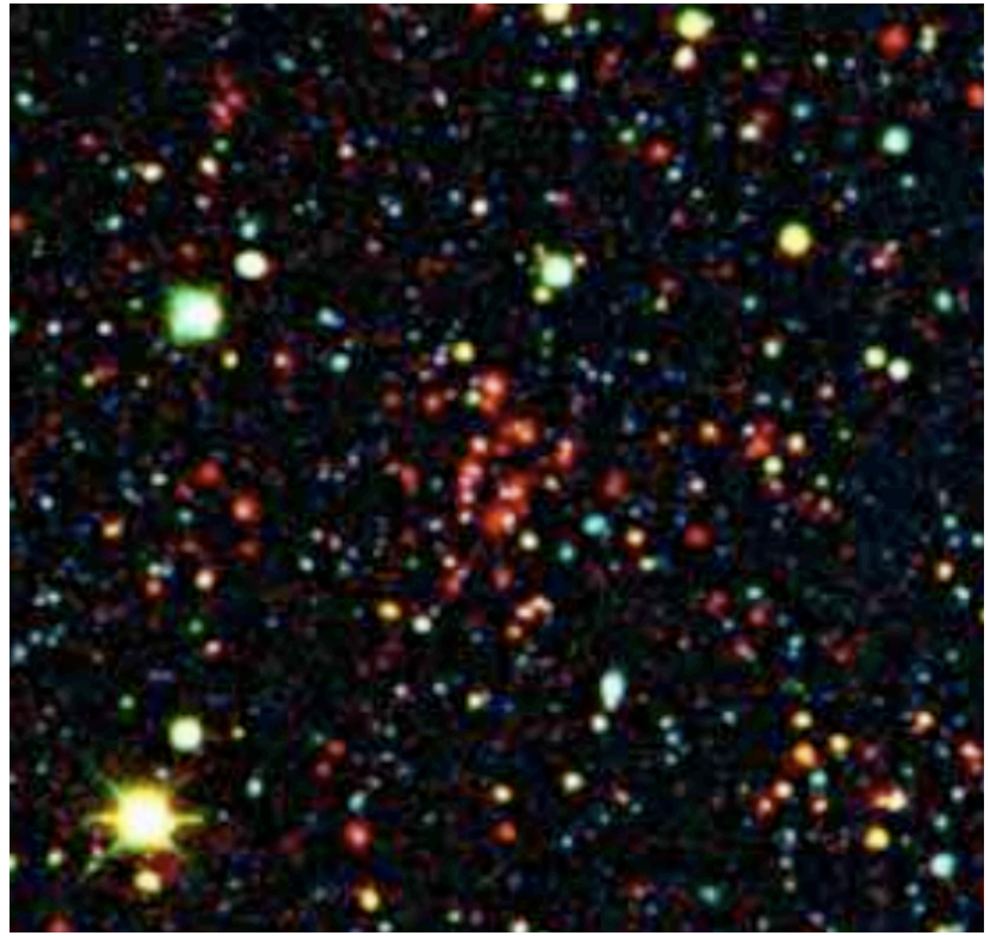

z = 0.29
SDSS maxbcg

z = 1.37
Spitzer IRAC

massive halo phenomenology: observable signal likelihoods

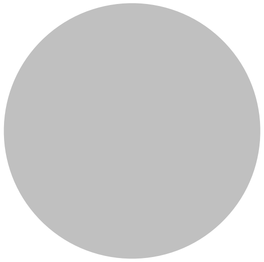

halo of
mass M
redshift z

=>

optical/lensing

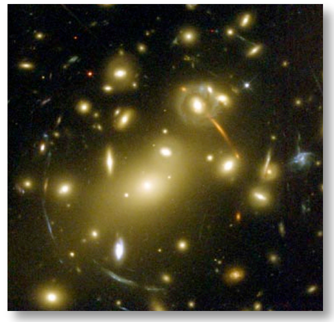

sub-mm

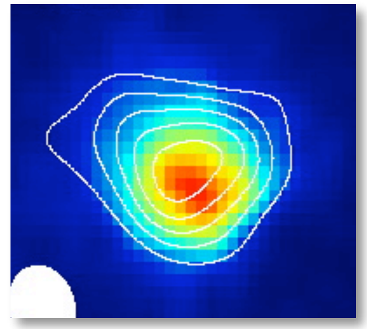

X-ray

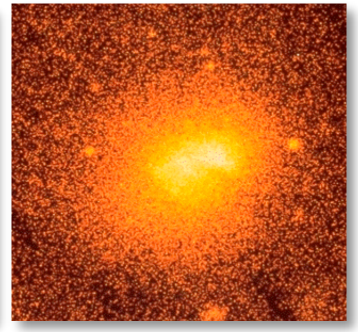

"Astrophysics 101"

1. Dimensional analysis => mean relations are power-laws

2. Central Limit Theorem => deviations are log-normal

the end